

NASA/TM–2014-218509



Design of the VISITOR Tool: A Versatile ImpulSive Interplanetary Trajectory OptimizeR

*Luca Corpaccioli and Harry Linskens
Science and Technology Corporation, Hampton, Virginia*

*David R. Komar
Langley Research Center, Hampton, Virginia*

July 2014

NASA STI Program . . . in Profile

Since its founding, NASA has been dedicated to the advancement of aeronautics and space science. The NASA scientific and technical information (STI) program plays a key part in helping NASA maintain this important role.

The NASA STI program operates under the auspices of the Agency Chief Information Officer. It collects, organizes, provides for archiving, and disseminates NASA's STI. The NASA STI program provides access to the NASA Aeronautics and Space Database and its public interface, the NASA Technical Report Server, thus providing one of the largest collections of aeronautical and space science STI in the world. Results are published in both non-NASA channels and by NASA in the NASA STI Report Series, which includes the following report types:

- **TECHNICAL PUBLICATION.** Reports of completed research or a major significant phase of research that present the results of NASA Programs and include extensive data or theoretical analysis. Includes compilations of significant scientific and technical data and information deemed to be of continuing reference value. NASA counterpart of peer-reviewed formal professional papers, but having less stringent limitations on manuscript length and extent of graphic presentations.
- **TECHNICAL MEMORANDUM.** Scientific and technical findings that are preliminary or of specialized interest, e.g., quick release reports, working papers, and bibliographies that contain minimal annotation. Does not contain extensive analysis.
- **CONTRACTOR REPORT.** Scientific and technical findings by NASA-sponsored contractors and grantees.

- **CONFERENCE PUBLICATION.** Collected papers from scientific and technical conferences, symposia, seminars, or other meetings sponsored or co-sponsored by NASA.
- **SPECIAL PUBLICATION.** Scientific, technical, or historical information from NASA programs, projects, and missions, often concerned with subjects having substantial public interest.
- **TECHNICAL TRANSLATION.** English-language translations of foreign scientific and technical material pertinent to NASA's mission.

Specialized services also include organizing and publishing research results, distributing specialized research announcements and feeds, providing information desk and personal search support, and enabling data exchange services.

For more information about the NASA STI program, see the following:

- Access the NASA STI program home page at <http://www.sti.nasa.gov>
- E-mail your question to help@sti.nasa.gov
- Fax your question to the NASA STI Information Desk at 443-757-5803
- Phone the NASA STI Information Desk at 443-757-5802
- Write to:
STI Information Desk
NASA Center for AeroSpace Information
7115 Standard Drive
Hanover, MD 21076-1320

NASA/TM-2014-218509



Design of the VISITOR Tool: A Versatile ImpulSive Interplanetary Trajectory OptimizeR

*Luca Corpaccioli and Harry Linskens
Science and Technology Corporation, Hampton, Virginia*

*David R. Komar
Langley Research Center, Hampton, Virginia*

National Aeronautics and
Space Administration

Langley Research Center
Hampton, Virginia 23681-2199

July 2014

The use of trademarks or names of manufacturers in this report is for accurate reporting and does not constitute an official endorsement, either expressed or implied, of such products or manufacturers by the National Aeronautics and Space Administration.

Available from:

NASA Center for AeroSpace Information
7115 Standard Drive
Hanover, MD 21076-1320
443-757-5802

ABSTRACT

The design of trajectories for interplanetary missions represents one of the most complex and important problems to solve during conceptual space mission design. To facilitate conceptual mission sizing activities, it is essential to obtain sufficiently accurate trajectories in a fast and repeatable manner. To this end, the VISITOR tool was developed. This tool modularly augments a patched conic MGA-1DSM model with a mass model, launch window analysis, and the ability to simulate more realistic arrival and departure operations. This was implemented in MATLAB, exploiting the built-in optimization tools and vector analysis routines. The chosen optimization strategy uses a grid search and pattern search, an iterative variable grid method. A genetic algorithm can be selectively used to improve search space pruning, at the cost of losing the repeatability of the results and increased computation time. The tool was validated against seven flown missions: the average total mission ΔV offset from the nominal trajectory was 9.1%, which was reduced to 7.3% when using the genetic algorithm at the cost of an increase in computation time by a factor 5.7. It was found that VISITOR was well-suited for the conceptual design of interplanetary trajectories, while also facilitating future improvements due to its modular structure.

List of Symbols

<u>Symbol</u>	<u>Definition</u>	<u>Unit</u>	<u>Subscript</u>	<u>Definition</u>
V_∞	Excess Velocity	km/s	<i>ib</i>	Inbound
α	Hyperbolic Turn Angle	rad	<i>ob</i>	Outbound
r	Radius	km	<i>tot</i>	Total
μ	Gravitational Parameter	km ³ /s ²	<i>p</i>	Periapsis
ΔV	Impulsive Velocity Change	km/s	<i>a</i>	Apoapsis
V	Velocity	km/s	<i>GA</i>	Gravity Assist
i	Inclination	rad	<i>esc</i>	Escape
a	Semi-Major Axis	km	<i>hyp</i>	Hyperbolic Orbit
φ	Rotation Angle	rad	<i>park</i>	Parking Orbit
Ω	Right Ascension Of The Ascending Node	rad	<i>RGA</i>	Resonant Gravity Assist
ω	Argument Of Periapsis	rad	<i>helio</i>	Heliocentric
n	Mean Motion	rad/s	<i>sun</i>	Of The Sun
R	Planet Radius	km	<i>pl</i>	Of The Planet
e	Eccentricity	[-]	<i>inert</i>	Inert Stage
J_2	J ₂ Spherical Harmonic Coefficient	[-]	<i>prop</i>	Propellant
P	Orbital Period	s	<i>pld</i>	Effective Payload
j	Integer Number Of Spacecraft Revolutions Around Sun	[-]	<i>pay</i>	Mission Payload
k	Integer Number Of Planet Revolutions Around Sun	[-]	<i>0</i>	Initial
M	Mass	kg	<i>i</i>	Generic Counter
I_{sp}	Specific Impulse	s	<i>j</i>	Generic Counter
ζ	Tankage Mass Fraction	[-]	<i>D</i>	Departure
ε	Inert Mass Fraction	[-]	<i>A</i>	Arrival
<i>MJD</i>	Modified Julian Date	days	<i>I</i>	Interplanetary
<i>TOF</i>	Time-Of-Flight	days	<i>grid</i>	Grid Search
<i>Δdate</i>	Difference In Date	days		

1. Introduction

The problem of trajectory optimization is one of the central topics in space mission design. This is especially true when considering interplanetary flight, in which it becomes one of the central drivers for the mission. Additionally, this is a problem with high degrees of complexity, in which there is no “easy” analytical way to approximate trajectories, even at a conceptual phase. Said problem almost always involves the optimization of a multivariate functions with several constraints.

This paper focuses on the need for sizing interplanetary trajectories rather than developing the best optimization possible. Here, the user is not necessarily after the absolute best possible trajectory but seeks to compute multiple cases rapidly, valuing computational efficiency over fidelity. Furthermore, for a sizing tool, it is essential to be able to obtain repeatable results such that the user can, for example, investigate the sensitivity of certain variables. This is a rather stringent requirement, which is almost never fulfilled when considering all modern efforts done in this area [1].

Furthermore, since a sizing tool should serve many purposes, it is important to obtain a modular program which is easily usable and modifiable by many without too much programming knowledge. Such capability would allow it to interface easily with other tools, and therefore serve a broader purpose.

This paper describes how the VISITOR tool works, and how it answers this specific need. It is divided in three main parts. The first shows how the trajectory aspects are modelled; then moves onto the optimization strategy used, and finally ends by benchmarking the results against several flown missions to ensure the program produces realistic trajectories.

2. Trajectory model

This section describes how each routine of the program is modeled, including how solution methods were implemented. First, the basic multiple gravity assist (MGA) patched conic formulation is described, which serves as a basic structure to the other subroutines. Then, the various additions to such basic model, which serve to more accurately simulate reality, are detailed. These are the inclusion of departure and arrival orbits in planetary space, the presence of potential deep space maneuvers (DSM's), the ability to perform more complex transfer orbits (multiple revolutions, resonant orbit gravity assist), the ability to rendezvous with asteroids, and a mass model which allows computing and updating spacecraft mass throughout the mission as elements are spent or added.

2.1 MGA Model

An interplanetary trajectory is defined here by a series of Keplerian arcs connecting together relevant nodes around the Sun. For now, such nodes are the planets themselves; however this is not always the case. Such arcs are initially determined by selecting a planetary sequence and the times of flight between each planet. The times of flight specify the date of each planetary encounter; in turn, a planetary ephemeris [2] [3] is used to determine the exact coordinates of the planets in three-dimensional space. The location of these nodes and the time of flight between them fully determines Lambert's problem [4], which is then solved using Gooding's method [5]. Thus, one obtains a series of connecting Keplerian arcs which the spacecraft must follow. Note that multiple-revolution transfers are also possible.

2.1.1 Patched Conic and Gravity Assist Model

After having determined the necessary transfer orbits to fly a determined trajectory, the first step is to patch them together at each of the nodes. This is done using the patched conic approximation [4]. The required change in velocity to go from one orbit to another is applied instantaneously as a powered gravity assist (GA) at the periapsis of each hyperbolic fly-by.

The known variables are therefore the incoming and outgoing heliocentric velocities at each node necessary to fly the Keplerian arcs. These in turn translate to an inbound and outbound excess velocity vectors $\mathbf{V}_{\infty,ib}$ and $\mathbf{V}_{\infty,ob}$ within the planet's sphere of influence. The unknowns to be calculated for such maneuvers are the hyperbolic periapsis radius and the ΔV magnitude of the powered assist. Together, these two variables must ensure that when the spacecraft arrives with $\mathbf{V}_{\infty,ib}$, it departs with $\mathbf{V}_{\infty,ob}$.

First, the angle between $\mathbf{V}_{\infty,ib}$ and $\mathbf{V}_{\infty,ob}$ is determined, which is the required turn angle α_{tot} to be provided by the hyperbola. Thus Equation (1) can be written as shown below.

$$\alpha_{tot} = \alpha_{ib} + \alpha_{ob} \quad (1)$$

In Equation (1), α_{ib} is the turn angle provided by the first half of the hyperbola, going from $\mathbf{V}_{\infty,ib}$ to periapsis, and α_{ob} is the turn angle of the second half of the hyperbola, going from periapsis to $\mathbf{V}_{\infty,ob}$. The simple relation for hyperbolic turn angle is then substituted in Equation (1), yielding Equation (2) for total turning angle of the powered gravity assist.

$$\alpha_{tot} = \sin^{-1} \left(\frac{1}{1 + \frac{r_p |\mathbf{V}_{\infty,ib}|^2}{\mu}} \right) + \sin^{-1} \left(\frac{1}{1 + \frac{r_p |\mathbf{V}_{\infty,ob}|^2}{\mu}} \right) \quad (2)$$

The transcendental Equation (2) is then numerically solved for hyperbolic periapsis. Note that since the outgoing and incoming V_∞ are potentially different in magnitude, two distinct hyperbola legs will be flown, with a common periapsis. Also note that, based on the planetary body in question, there is an absolute minimum periapsis radius that can be flown due to practical constraints (atmospheres and solid surfaces), hence anything below this limit makes the trajectory impossible to fly.

Having determined the periapsis radius, the last step is to find the required ΔV of the powered assist. This is readily computed by subtracting the magnitudes of periapsis velocities of the two hyperbola legs as described in Equation (3).

$$\Delta V_{GA} = \sqrt{V_{\infty,ib}^2 + V_{p,esc}^2} - \sqrt{V_{\infty,ob}^2 + V_{p,esc}^2} \quad (3)$$

Thus, after having selected a planetary combination, and having computed all the periapsis radii and powered assist magnitudes, the Keplerian arcs described in Section 2.1 can be flown (provided the radii are above the pre-set minima).

2.1.2 Deep Space Manuever (DSM) Model

DSMs can significantly improve a trajectory's feasibility; in fact, several past missions have flown an MGA-1DSM trajectory, wherein one DSM was given along certain arcs [6] [7]. It is therefore important to be able to accurately simulate this. A schematic of the model used is shown in Figure 1.

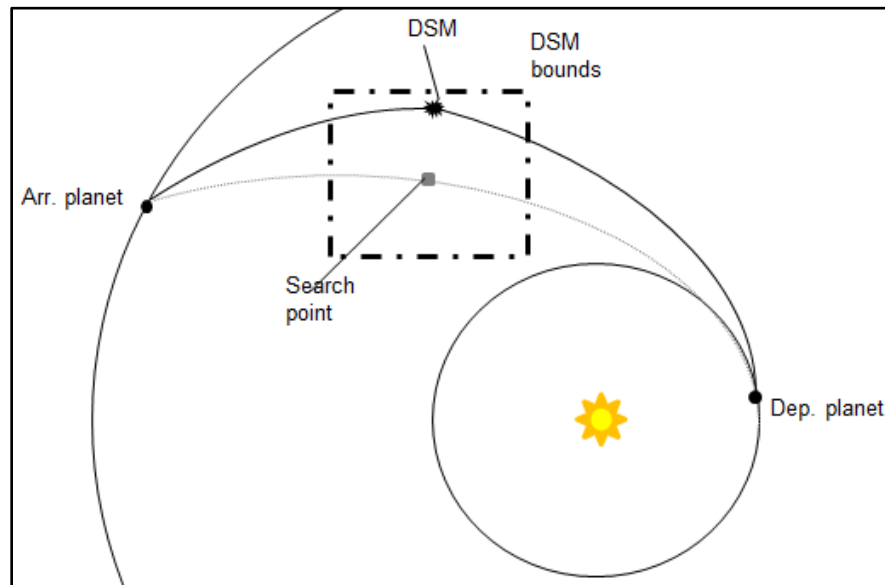


Figure 1: Schematic of DSM model

At first, an initial guess for a time of flight is used to compute the unperturbed trajectory with no DSM, corresponding to the gray trajectory in Figure 1. Next, a point along this trajectory is chosen based on a percentage of the time of flight, known as the search point. For example, if the time percentage is set to 40% and time of flight is 300 days, the search point is set to the location on the unperturbed trajectory after 120 days, indicated in Figure 1 by the gray square. At this point, bounds are placed around the search point, which form a “cube” around it (although in the planar figure they are shown as a square).

Now the DSM computations can begin: a point is chosen inside this search space, referred to here as the DSM point, and Lambert's problem is solved, connecting it to the departing planet in the time allocated by the time percentage (the 120 days). Next Lambert's problem is solved again, connecting the DSM point with the arrival planet in the remaining time of flight (in this case 180 days). These two Keplerian arcs are patched by a DSM burn to form a new trajectory, shown in black in Figure 1. The results would then have to be further optimized by choosing better times of flight, DSM search point along the trajectory, and point inside the search space.

A point of note is that DSMs are generally modeled by varying the departure velocity from a planet rather than varying the mid-point [8]. The method described in this paper was chosen to allow better estimation of the exact position of the DSM through linear constraints (see Section 4.3), which in turn can better simulate mission restrictions. For example, the spacecraft may want to avoid certain regions (asteroid presence, proximity to the sun etc...), which is easily done with such a formulation. Furthermore, this implementation is seldom used, and therefore it can allow for future verification with more popular simulation methods.

2.2 Planetary Operations

One of the major additions to the MGA model described in Section 2.1 is the analysis of the trajectory within planetocentric space upon departure and arrival. Doing this allows the full ΔV requirement of the mission to be determined, which can then be used for more accurate vehicle sizing. In order to do this, the periapsis distance r_p , apoapsis distance r_a , and inclination i of the departing or arriving orbit must be specified by the user (also known as parking and target orbit respectively). Choosing this incomplete set of orbital elements allows the user to define the most important characteristics of the orbit for the mission at hand, while allowing simple analytical methods to be used to determine burn magnitudes.

A number of different types of departure and arrival procedures can be analyzed, which will have a different impact on the final cost function. These procedures are summarized in the following subsections. For all cases, it is assumed that burns to change velocity are purely tangential burns. Burns to change inclination will contain a component out of the orbital plane. It should be noted that for sections 2.2.1 and 2.2.2 only the departure from a parking orbit to a hyperbolic trajectory is described, as the arrival is simply the reverse of this process.

2.2.1 One-Burn Transfers

The simplest form of planetary operations is to perform a one-burn transfer. During such a maneuver, the spacecraft transitions directly from the parking orbit to the hyperbolic escape trajectory, using only a single tangential ΔV at periapsis. In applying this form of analysis, the orientation of the escape trajectory with respect to the target orbit is disregarded, and it is thus assumed that the orbits are correctly aligned. As such, one-burn transfers are only realistic forms of analysis if there are no requirements on the orientation of the parking or target. The ΔV required for the one-burn transfer is given by the vis-viva equation, shown in Equation (4) [4]. In general, this equation will hold for all planar velocity change maneuvers.

$$\Delta V = \sqrt{\mu \left(\frac{2}{r_p} \right) - \left(\frac{1}{a_{hyp}} \right)} - \sqrt{\mu \left(\frac{2}{r_p} \right) - \left(\frac{1}{a_{park}} \right)} \quad (4)$$

2.2.2 Bi-elliptic Transfers

In order to simulate the departure from an orbit with a specified inclination around a specified planet, bi-elliptic transfers can be used. A bi-elliptic transfer will transition from the

parking orbit to the escape trajectory or vice versa with four burns, through an intermediate orbit with a high apoapsis [4]. Performing the inclination change at a high altitude will dramatically reduce the amount of ΔV required. The burn sequence is as follows: burn at periapsis of parking orbit to raise apoapsis, burn at apoapsis to set departure hyperbolic periapsis, burn at equatorial crossing to set polar inclination, and burn at new periapsis to enter hyperbolic escape. Each of these will be explained in detail.

The amount of ΔV required to rotate the orbit over an arbitrary angle φ can be determined using Equation (5) [4].

$$\Delta V = 2V \sin(\varphi/2) \tag{5}$$

The optimal location to change the inclination of the orbit is at apoapsis, as the velocity is lowest at this point. However, since inclination changes must be performed at equatorial crossing, this optimal solution can only be achieved if the line of apsides lies in the equatorial plane [4]. In this case, the second and third burns occur simultaneously, thus becoming a three burn transfer.

If this is not achievable (argument of periapsis is not 0), it is desirable to approach this condition as much as possible by choosing the orbit orientation such the velocity is as low as possible at the equatorial crossing. This, in turn, implies that the crossing must occur at the highest possible altitude. The latter is achieved by setting the inclination of the departure hyperbolic orbit to 90° . Then, the inclination change burn is performed upon crossing the equatorial plane, which is visualized in Figure 2.

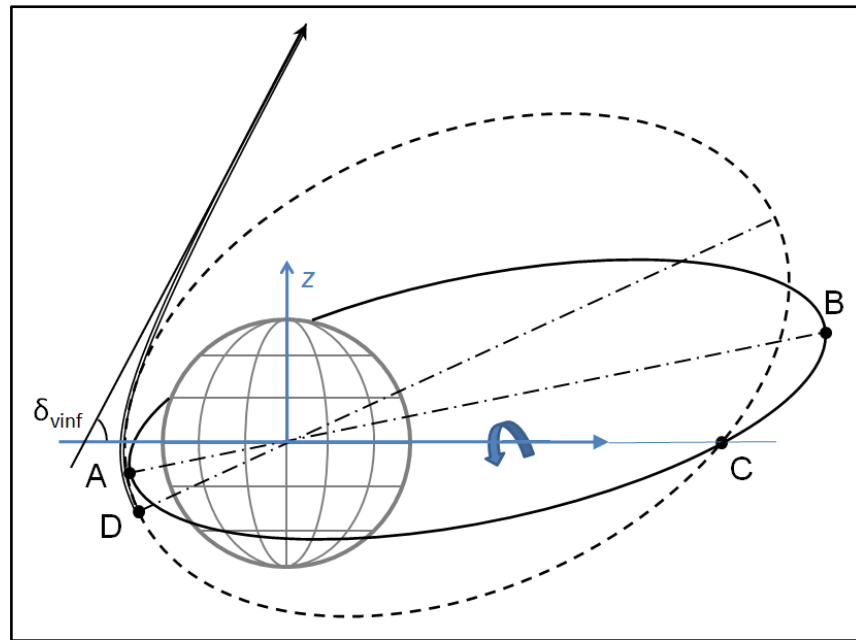


Figure 2: Schematic of suboptimal bi-elliptic inclination change

In Figure 2, a departure condition is considered in which the declination $\delta_{v_{inf}}$ of the $V_{\infty,ob}$ vector and the periapsis altitude, necessitate a bi-elliptic transfer. Initially, the spacecraft is in a parking orbit with specified r_p , r_a , and i . At periapsis of the parking orbit, a burn is performed to raise the apoapsis, which corresponds to point A in Figure 1. This puts the spacecraft in a highly elliptical clockwise orbit in the same plane as the parking orbit, shown by the solid line (the parking orbit is not shown). Note that the line of apsides does not lie in the equatorial plane.

At point B, a burn is performed to change the periapsis altitude, if the parking and hyperbolic periapsis altitudes are different. Then, at the equatorial crossing near apoapsis, at point C, the third burn is performed to rotate the orbit around the line of nodes, changing the inclination to 90° , resulting in the orbit shown by the dashed line. Finally, at point D, the departure burn is performed. From this inclination, any $\delta_{v_{inf}}$ can be targeted. There is a dependence on the argument of periapsis, so it is assumed that the argument of periapsis of the initial orbit is set such that this maneuver is possible.

While this solution is suboptimal, it allows the burn magnitudes to be found using consistent analytical relations, maintaining the fast operating speed of the tool. Upon arrival the same method is used, but the steps are performed in reverse.

2.2.3 Apo-Twist Transfers

When a round trip mission is simulated (an arrival followed by a departure), the orientation of the parking orbit around the target planet becomes important for determining accurate ΔV values. It is desirable to line up the inbound and outbound asymptotes during the stay, such that $\mathbf{V}_{\infty,ib}$ and $\mathbf{V}_{\infty,ob}$ can be achieved in minimal ΔV . A method to do this is based on a single rotation about the line of apsides to align an inbound and an outbound escape trajectory, known as apo-twist [9]. This rotation is then accomplished by a single burn at apoapsis at the correct time during the stay.

This method uses B-plane targeting to align the periapsis vectors of the inbound and outbound hyperbola legs, for a set r_p and r_a of a parking orbit, such that only one tangential burn at arrival and one tangential burn at departure is necessary in addition to the apo-twist maneuver itself. The angle between the angular momentum vectors of the resulting hyperbolic trajectories then forms the angle to rotate at apoapsis. The ΔV required for this rotation can then be determined using Equation (5). Thus, by choosing the correct B-plane arrival and departure point, given a target parking orbit, it is possible to align the inbound and outbound excess velocities with three burns.

Additionally, precession due to the J_2 effect is taken into account. This secularly affects the right ascension of the ascending node Ω and argument of periapsis ω , the behavior of which are governed by Equation (6) [9]. This solution methodology requires the use of numerical solvers, and is also not guaranteed to find a solution. However, to disregard the J_2 effect in this case is not acceptable, and thus the effect thereof is included in the simulation. The full implementation of apo-twist is too complex to be fully detailed here; however it follows the method described in Landau [9], the source of which is in the bibliography.

$$\begin{aligned}\dot{\Omega} &= -\frac{3}{2}n\frac{J_2R_p^2}{a^2(1-e^2)^2}\cos(i) \\ \dot{\omega} &= \frac{3}{4}n\frac{J_2R_p^2}{a^2(1-e^2)^2}(1-5\sin^2 i)\end{aligned}\tag{6}$$

2.2.4 Aerocapture

It is also possible to consider an aerocapture maneuver upon arrival. This allows the spacecraft to reach the target apoapsis using aerodynamic drag instead of a rocket burn. At present, no tool is integrated within VISITOR to allow for the analysis of such maneuvers. However, a switch exists in the code which can be used to incorporate an external aerocapture tool. This switch simply sets the cost function for the arrival phase to zero.

2.2.5 Low-Thrust Departure Asymptote Alignment

An option also exists to use low-thrust propulsion to improve the energy state of the parking orbit around the departure planet, and to align this with the outbound hyperbola. As with aerocapture and EDL, the analysis for this is independent of the variables used in the evaluation of the interplanetary, allowing this analysis to be performed post-optimization. Also, it has not been integrated into VISITOR itself, although the resulting orbit can be input as a parking orbit at departure. Furthermore, as for apo-twist, the full description is too long to be included here. It follows the methods by Gefert and Hack [10], the source of which is in the appendix.

The method used is based on analytical in-plane steering angle solutions to four subsequent control laws [10]. First, the semi-major axis of the initial orbit is raised through tangential thrusting. Second, the argument of periapsis is rotated to align the orbit properly. Then, the apoapsis is raised while keeping the periapsis constant. Finally, the eccentricity is maximized, while respecting a minimum periapsis distance. For each phase, the corresponding control law, as a function of true anomaly, is applied to the steering angle, and the equations of motion are numerically integrated. Both eclipse and precession due to J_2 can be taken into account.

Since the trajectory must be numerically integrated, this analysis is rather slow. However, it does represent a mass-efficient method for improving the energy state upon departure, and therefore represents a valuable sizing tool.

2.4 Resonant Gravity Assist Model

A special class of GA trajectories occurs when the initial and target planets are the same and the phase angle between them is exactly 2π . At this point, Lambert's problem does not have a unique solution, as there are infinitely many solutions connecting the same point in a given period. However, such trajectories have been used on a number of previous missions (e.g. the Galileo [11], Rosetta [6], and MESSENGER [12] missions), so it was chosen to include the possibility for this special case in the overall analysis.

Two possible trajectories are considered: Gravity Assist–Resonant Gravity Assist (GARGA) trajectories and Departure–Resonant Gravity Assist (DRGA) trajectories. Both suffer from the same limitation in the solution to Lambert's problem, but require slightly different solution methodologies. These will be discussed in the subsequent subsections.

2.4.1 Gravity Assist–Resonant Gravity Assist (GARGA) Trajectories

The basic problem of GARGA trajectories is illustrated in Figure 3. In essence, it is desired to change the heliocentric velocity from V_{ib} to V_{ob} . However, this might not be possible in a single pass, if the turn angle required to do so is too large. Thus, an intermediate resonance trajectory is flown, splitting the required velocity change over two GA maneuvers.

The initial heliocentric velocity results in an initial inbound excess velocity at the planet ($V_{\infty,ib}$), as seen in Figure 3. During the first GA, the excess velocity vector is changed from $V_{\infty,ib}$ to $V_{\infty,RGA}$. Since the planet is encountered at the same position in the resonant orbit at both GA maneuvers, the heliocentric velocity vector of the spacecraft at the beginning and at the end of the resonance trajectory will be the same. Thus, after the resonance orbit (an integer amount of planet periods later), the inbound excess velocity at the planet will also be $V_{\infty,RGA}$. The second GA maneuver then changes this velocity to $V_{\infty,ob}$. Note that the two periapsis altitudes $r_{p,ib}$ and $r_{p,ob}$ are both unknown, and can be different.

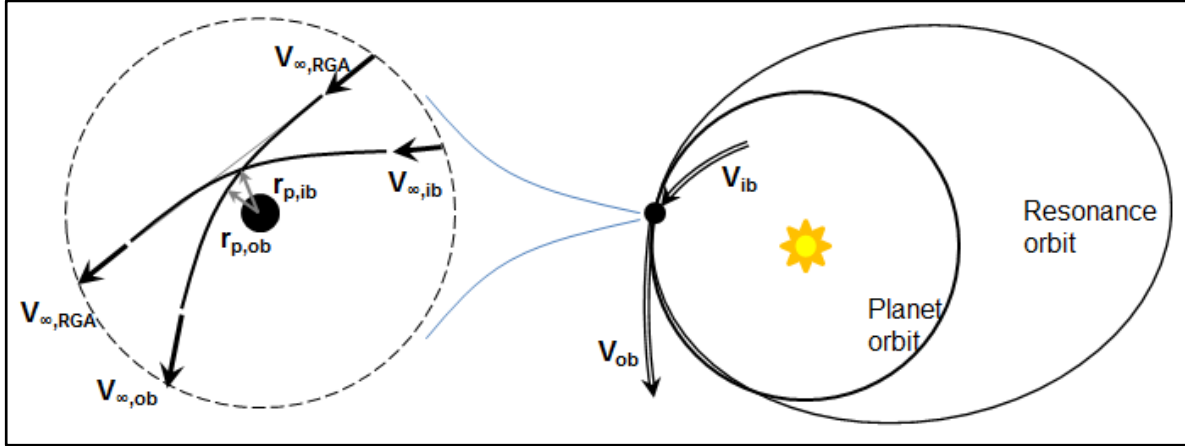


Figure 3: Schematic of RGA model. Left is planetocentric space, and right is heliocentric space.

The magnitude of the heliocentric velocity which must result from $V_{\infty,RGA}$ is also known. This results from the fact that the resonant orbit has a specified semi-major axis a_{helio} dependent on the user-input resonant ratio $j:k$, with j being the number of revolutions performed by the spacecraft and k being the number of revolutions performed by the planet. This semi-major axis is given in Equation (7), with P_{pl} being the orbital period of the planet

$$a_{helio} = \sqrt[3]{\mu_{sun} \left(\frac{j \cdot P_{pl}}{k \cdot 2\pi} \right)^2} \quad (7)$$

By extension, the excess velocity vector $V_{\infty,RGA}$ will also be identical at both planetary encounters, due to the patched conic approximation. Thus, for a certain choice of $V_{\infty,RGA}$, it is possible to solve for the periaxis distance $r_{p,ib}$ and $r_{p,ob}$ of each GA maneuver. This is done in the same fashion as described in Section 2.1.1. A numerical method is then used to solve for the $V_{\infty,RGA}$ vector, such that the total ΔV for both maneuvers is minimized.

2.4.2 Departure–Resonant Gravity Assist (DRGA) Trajectories

The basic problem for DRGA trajectories is essentially identical to that of GARGA trajectories: the unknown excess velocity vector $V_{\infty,RGA}$ must be found such that the ΔV of the maneuvers is minimized. However, since DRGA trajectories start with a departure phase, there is no inbound heliocentric velocity V_{ib} . As such, DRGA trajectories will minimize the magnitude of the GA burn, as a departure burn is generally provided by a separate upper stage and would thus provide unrealistic numbers for sizing the spacecraft itself. Naturally, although this burn is not kept into account in finding optimal resonant orbit, it is instead taken into account in the total cost function.

2.5 Rendezvous Model

In the context of this paper, rendezvous refers to the heliocentric position and velocity of the spacecraft matching that of a target body. While this can in principle be performed for any celestial body, including the major planets, it is most useful when applied to celestial bodies with a negligible gravity field, i.e. asteroids or comets. Examples of missions flown to comets or asteroids include Rosetta or NEAR Shoemaker [13].

The actual analysis of a rendezvous trajectory is straightforward: given the departure and arrival epochs, and the state of the initial planet and the target, a Lambert solution is found between the two. To match the velocity, a burn is performed at arrival with the object, the vector of which is simply given by the difference between the final velocity in the transfer orbit and the velocity of the target. This burn is then included in the optimization total cost function which will be discussed in Section's 4 and 5 below.

Thus, the most important element in the rendezvous model is the ability to retrieve the state of the target body. To do this, the JPL HORIZONS ephemeris computation is used [3], together with the SPICE library [2], in order to read out the data. The binary ephemeris files for minor solar system bodies which are read by SPICE can be generated for free on-line [14].

2.6 Mass Model

An important improvement over most trajectory optimization tools is the integration of a mass model in VISITOR. This allows it not only to minimize for total mission ΔV , but it can also minimize initial mass for a certain amount of payload. The basic mass model considers a single stack of i high-thrust propulsion stages and j payload elements. For each stage, the specific impulse I_{sp} and the inert mass ratio ϵ , defined as $M_{inert}/(M_{inert}+M_{prop})$, is specified by the user, with ϵ being either constant, or a function of the propellant mass. Per payload element, the user must also specify when it is added to or jettisoned from the stack, allowing elements to be on- or off-loaded mid-mission. Finally, it is specified which stage performs which burns. Note that one stage can perform multiple burns, but the stages must be used sequentially.

The mass iteration for a single stack element is detailed in Figure 4. In this figure, a sample case is taken where a single stage performs three burns. The third burn is evaluated first, and the corresponding propellant mass $M_{prop,3}$ and inert mass $M_{inert,3}$ are found with the prescribed payload mass $M_{pay,3}$. Then, the second burn is evaluated, using $M_{prop,3}$ summed with the new prescribed payload mass $M_{pay,2}$ as the total effective payload mass $M_{pld,2}$. A new inert mass $M_{inert,2}$ is found, and if this is different from $M_{inert,3}$, the found value is fed back to the iteration loop of the third burn. Once the two inert masses match, the analysis is stepped forward to the first burn. This process repeats across all stages until final convergence. If a multi-stage stack is considered, the resulting total mass forms the payload for the next stage.

Note that the tankage mass fraction ζ , defined as M_{inert}/M_{prop} , is used instead of ϵ for more convenient notation; the conversion between the two is defined in Equation (8).

$$\zeta = \epsilon / (1 - \epsilon) \quad (8)$$

While the mass model described is quite basic, it has been designed to be easily replaced later on with other, more detailed mass model, once these become available. The importance is that it is included within the optimization routine, and thus the final solution will be mass-optimal.

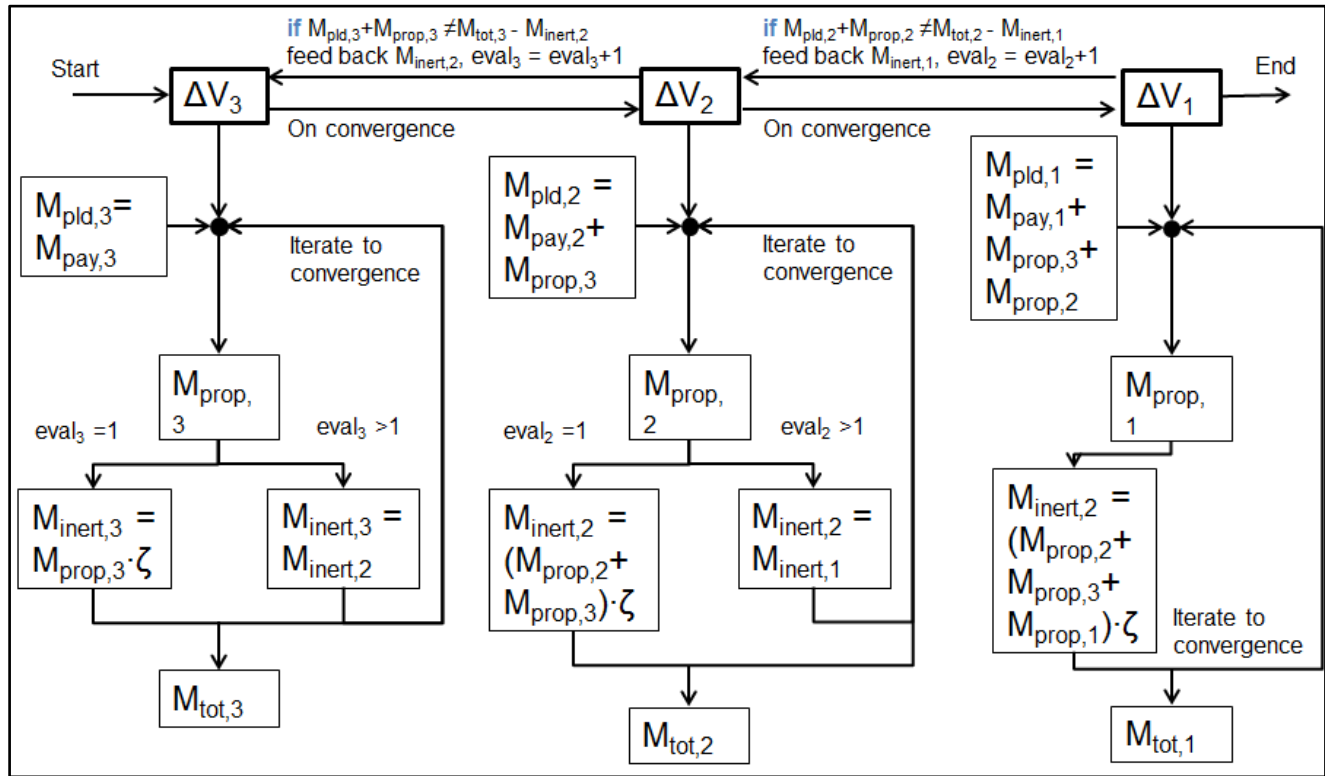


Figure 4: Diagram of mass model iteration for a three-burn, one-stage spacecraft.

3. Choice of programming language

This section discusses the chosen programming language, and evaluates its usefulness when compared to other options. The choice was made to write VISITOR in MATLAB, which has implications for both computation speed and development time. First, previous choices for programming languages used in solving the interplanetary trajectory problem will be discussed, followed by arguments for the choice of using MATLAB. Finally, some examples will be given on its practical use.

3.1 Previous Efforts

Many interplanetary trajectory optimization tools found in the literature use the C++ or FORTRAN languages to model the problem. Traditionally, these languages allow the computations to be performed more quickly than with MATLAB [15]. However, some aspects of these languages may make them less attractive for rapid software development. The main consideration is the lack of integrated routines within the standard packages and libraries, necessitating that many of the tools used must be coded by the user. This implies that a larger skill set may be required to be able to write the tool efficiently. Also, the structuring of code requires a lot of user specification in order to run properly, e.g. every variable must be predefined as a certain type.

3.2 Advantages of MATLAB

MATLAB has a number of advantages over the commonly used C++ and FORTRAN languages. It is a so-called fourth-generation language, which adds an extra layer of abstraction above the level used in third-generation languages, of which C++ and FORTRAN are examples [15]. Thus, structuring of code requires less user specification, and standard packages and libraries contain many integrated routines. The resulting ease of programming significantly reduces development time and guarantees robustness, since many basic routines are preprogrammed and thus thoroughly verified. This leaves a lot more time for post-evaluation and further improvements, rather than writing the actual tool. Furthermore, these routines are available on almost all copies of MATLAB, whereas other C++ and FORTRAN libraries are often not readily available.

As previously mentioned, MATLAB contains many integrated routines. Examples of routines used in VISITOR and other general advantages are summarized below.

- It is an engineering tool, meaning it comes equipped with a large number of useful basic functions. Examples include numerical solvers (e.g. "fsolve.m"), and efficient integrators (e.g. "ode45.m").
- Its vector-based operations aid in many large computations, as well as helping to avoid slow loops. Furthermore, it possesses a large number of useful vector and matrix functions, such as the ability to reorder and reshape vectors (e.g. "min.m", "reshape.m"). This also helps when dealing with frame transformations and vector rotations, for example, the command to convert a rotation matrix to axis-angle formulation (e.g. "vrrotvec2mat.m").
- There are many packages that come with it, which further enhance engineering capability. The most useful one considered here is the Optimization package. This comes with several optimizers, such as genetic algorithms and gradient-based methods. These are extremely complex routines which could take significant amounts of time to replicate (in fact, there is an entire field in engineering dedicated

- to this subject). The user can thus harness this entire body of knowledge with simple function calls (e.g. "ga.m", "fmincon.m").
- Ample shareware availability. Even if MATLAB does not have a pre-made function, it is often the case that freeware is available to solve a particular problem (even in the case of astrodynamics). Examples include Lambert problem solvers, Kepler equation solvers and Cartesian to Keplerian converters. These do need to be verified, however they are often efficient, and again save programming efforts.
 - MATLAB is extremely popular, and is available to anybody who purchases a license. This means that VISITOR could be run by a large number of engineers which increases its user base, and possibilities of improvement.
 - The SPICE library is easily available in MATLAB through MICE routines [2], which makes implementation of planetary ephemerides and asteroids extremely easy, as well as simplifying the process of heliocentric to planetocentric frame transformation.
 - MATLAB interfaces well with other popular programs; examples include Microsoft Excel, Visual Basic for Applications (VBA) and Satellite ToolKit (STK). Furthermore, it is possible to easily convert MATLAB script to C script via the MATLAB Coder [16].

It must be noted that most capabilities summarized above could be implemented in other languages than MATLAB. However, the routines that are built into MATLAB have been developed and improved by experts in the field, and therefore can be said to be extremely robust and efficient. This speeds up VISITOR remarkably, as well as significantly cutting on development time.

4. Problem Formulation

In this section, the method in which the interplanetary trajectory problem was formulated will be detailed. The formulation described is then used in the numerical analysis of the problem, which will be discussed further in Section 5. First, the simplified and full problem formulations are explained followed by a summary of the constraints used to bound the search space.

4.1 Simplified Problem Formulation

The simplified problem formulation only considers the basic interplanetary trajectory, and is set up as a multidimensional static optimization problem. This formulation allows for the analysis of the MGA model, along with the possibility for RGA trajectories. As such, it excludes all forms of planetary operations and DSMs, and it is thus requires to use the excess velocities in the cost function, along with GA burns. It is possible to specify which planets' excess velocity should be taken into account in the cost function.

A result of this formulation is a problem of which the dimension is relatively low: the control vector \mathbf{x}_s consists only of the initial date (in MJD) and the time-of-flight (in days) for each leg. Thus, a relatively complex trajectory such as the EVVEJS trajectory flown by Cassini can be analyzed using only six variables. The structure of \mathbf{x}_s is shown for a trajectory with i legs in Equation (9).

$$\bar{\mathbf{x}}_s = [MJD_0 \quad TOF_1 \quad TOF_2 \quad \dots \quad TOF_i]^T \quad (9)$$

4.2 Full Problem Formulation

With the full problem, all elements detailed in Section 2 are incorporated in the problem formulation. Doing so results in a need to expand the control vector, increasing the dimensionality of the problem.

First, the time-of-flight for each leg is split up into three separate time-of-flights: one allocated to the planetary departure phase (T_D), one allocated to the interplanetary phase (T_I), and one allocated to the planetary arrival phase (T_A). This allows more favorable geometries in heliocentric space to be traded off against more favorable geometries in planetocentric space. For certain legs, the departure or the arrival time-of-flight is set to zero, for instance during GA maneuvers or one-burn departures or arrivals.

Second, to account for DSMs, four variables are added to the control vector per DSM performed: the time at which the DSM occurs in its leg (T_{DSM}) and the three Cartesian coordinates of the DSM location.

The final structure of the control vector of the full problem \mathbf{x}_f is shown in Equation (10), for an example with i legs and j DSMs.

$$\bar{\mathbf{x}}_f = \begin{bmatrix} MJD_0 & TOF_{D,1} & TOF_{I,1} & TOF_{A,1} & \dots & TOF_{D,i} & TOF_{I,i} & TOF_{A,i} & \dots \\ \dots & TOF_{DSM,1} & x_{DSM,1} & y_{DSM,1} & z_{DSM,1} & \dots & TOF_{DSM,j} & x_{DSM,j} & y_{DSM,j} & z_{DSM,j} \end{bmatrix}^T \quad (10)$$

As a result of the use of the full problem formulation, a number of different cost functions can be selected. As with the simplified problem, it is possible to formulate the cost function in terms of excess velocities along with GA and DSM burns. Alternatively, planetary departure and arrival delta- V 's can be used instead of excess velocities. Finally, it is possible to use the burn magnitudes and the mass model to express the cost function in terms of initial stack mass.

4.3 Constraints on Problem

Any static optimization problem $\min F(\bar{x})$ can contain particular constraints. These are functions of the control variables that must be satisfied. In turn, these are divided into equality constraints $g(\bar{x}) = 0$ and inequality constraints $h(\bar{x}) \leq 0$. A further distinction can be made, wherein they can be said to be linear or non-linear, which occurs if the functions $g(\bar{x})$ or $h(\bar{x})$ are either linear or not. This is an important distinction to make, as numerical optimizers have particular difficulty in enforcing nonlinear constraints, especially when the function is complex and not easily differentiable. It is crucial to the speed of a program to be able to find fast solutions to such constraints.

4.3.1 Penalty functions

A popular method of dealing with nonlinear constraints is through penalty functions [17]. This is when the optimizer does not try to enforce the nonlinear constraint function, but rather it evaluates it, and determines whether the current combination of control variables is violating the constraint or not. If it is, the cost function is “artificially” increased by applying a penalty term. This will force the optimizer to shy away from that combination of state variables and seek an area where the constraints are no longer violated.

Throughout the program, linear penalty functions are used to replace nonlinear constraints. Given the problem $\min F(\bar{x})$, with nonlinear constraint $h(\bar{x}) \leq 0$, a candidate solution is used to evaluate $h(\bar{x})$. If this is found to be outside the constraint, the optimization problem changes to $\min(k_1 F(\bar{x}) + k_2)$, where the constants k_1 and k_2 are to be selected. Usually they have to be large enough (in the order of 10^3 - 10^4) such that no solution outside the constraint could possibly be better than a solution inside. Thus if the cost function appears to be extremely large ($<10^3$) it means a nonlinear constraint is violated, and the trajectory is infeasible.

There are some disadvantages in using this method. First, the function cannot distinguish when a nonlinear constraint is violated, so it will evaluate more points than it needs to, and the user must decide whether an optimizer is within constraints or not. In addition, by changing the cost function upon violation of the constraints, large discontinuities are added to the problem, which makes the function more “jagged” and hard to differentiate.

4.3.2 Constraints on the simplified problem

All the constraints used on the simplified problem are found in Table 1. Three different types of constraints are considered, each of which can fall in three separate categories. The types of constraint considered are bounds, linear constraints, and nonlinear constraints. Bound constraints are a special type of linear constraint where $x_i \leq 0$.

The three categories which can be defined are ceiling, floor, or two-side. A ceiling indicates a situation in which the function is not allowed to be greater than the constraint. Conversely, a floor indicates that the function is not allowed to be smaller than the constraint. Finally, a two-side indicates that both a ceiling and a floor are used. Note that bound constraints are necessary to some optimizers, as these require a limited search range (see Section 5).

Table 1: Active constraints on simplified problem

Constraint name	Explanation	Type
Departure date	Set constraints on desired departure date.	Bound, Two-side
Times of flight	Set constraints on desired time of flight for each leg	Bound, Two-side
Minimum heliocentric distance	Spacecraft must not come closer than a particular limit to the Sun*	Nonlinear, Floor
Minimum flyby periapsis	Constraint on how close spacecraft can perform a planet flyby	Nonlinear, Floor
Excess velocity	Bound excess velocity around any planet*	Nonlinear, Two-side
Max total flight time	Ensure the total flight time of all the legs combined is lower than a threshold*	Linear, Ceiling
<i>* constraint can be turned off by user</i>		

4.3.3 Constraints on the full problem

The full problem imposes a few additional constraints to those used for the simplified problem. These additional constraints are shown in Table 2. Note that the constraints from Table 1 are also still valid. Naturally the first two constraints in Table 2 are only used if the trajectory uses either DSMs or apo-twists.

Table 2: Added active constraints on full problem

Constraint name	Explanation	Type
Heliocentric DSM distance	Impose a minimum heliocentric distance that the spacecraft must keep during a leg with a DSM*	Nonlinear, floor
Apo-twist	Alignment of periapsis vectors in apo-twist. The constraint is violated if the difference between the periapsis vectors is more 50km*.	Nonlinear, ceiling
Total leg time-of-flight	The sum of the departure, interplanetary, and arrival phases must match the assigned total leg time-of-flight.	Linear, ceiling
<i>* constraint can be turned off by user</i>		

5. Optimization Strategy

This section describes the optimization strategy used for the program. As already noted in Section 4.1 and 4.2, the complete trajectory analysis can be reduced to a static optimization problem (a simplified and a full model). This section will explain which optimizers have been found to yield the best results, and how they are used. It is assumed that the reader is familiar with typical optimization techniques; therefore this paper will not go in much detail explaining how these work.

5.1 Grid Search

A grid search is perhaps the simplest type of optimization. It involves discretizing each variable of the control vector into nodes, usually regularly spaced from the lower bound to the upper bound. This gives the resemblance to a grid (or hyper grid, if the problem is multidimensional) [18]. Then, each possible combination of variable is computed, and the lowest cost function value is taken as best.

5.1.1 Implementation within the program

MATLAB does not possess built-in grid search routines. However, its capability to perform fast vector operations was used to accelerate the process. Within the program, the user specifies the grid resolution desired for each of the variables (departure date and times of flight). The program then creates N vectors (where N is the number of variables of the problem), each containing the regularly spaced grid points.

An example is shown in Equation (11), where the control vector is made up of two variables: departure date (MJD_0), and one time of flight (TOF_1). Furthermore, bounds are given to each of the variables (note that for departure date, the MJD formulation is used).

$$\begin{aligned} \bar{X} &= [MJD_0, TOF_1] \\ 338 &< MJD_0 < 538 \\ 150 &< TOF_1 < 250 \end{aligned} \quad (11)$$

Assuming the grid resolution is 100 days for the departure date, and 50 days for the time of flight, the grid vectors shown in Equation (12) are obtained

$$x_{grid,MJD_0} = \begin{bmatrix} 338 \\ 438 \\ 538 \end{bmatrix}, x_{grid,TOF_1} = \begin{bmatrix} 150 \\ 200 \\ 250 \end{bmatrix} \quad (12)$$

At this point, the program makes use of MATLAB's in built command "combvec.m". This tool combines any number of vectors and returns a matrix with every possible combination of the elements (referred to here as the combinations matrix). In this example, the output would be Equation (13).

$$x_{grid,tot} = \begin{bmatrix} 338 & 338 & 338 & 438 & 438 & 438 & 538 & 538 & 538 \\ 150 & 200 & 250 & 150 & 200 & 250 & 150 & 200 & 250 \end{bmatrix} \quad (13)$$

As can be seen, the columns provide all the combinations of control vectors to be computed in the grid search. The advantage of using this method is that MATLAB is able to very quickly

generate this combinations matrix, which can contain hundreds of thousands of columns. This circumvents the problem of having to use many nested loops, which are notoriously slow to run.

The final step is simply to take each column and run it through the function, and determine the best point(s). This will only require one loop.

5.1.2 Notes on the grid search

Despite being a global optimization strategy, it is well known that a grid search is rather slow to run, since it has to go through every possible combination of variables. This also means that it suffers from the classic curse of dimensionality [19], where the number of combinations rises exponentially with the number of variables. Thus, the more Keplerian arcs a problem has, the longer the grid search will take without sacrificing grid resolution. It is therefore advisable to reduce the number of variables as much as possible when using this technique.

A useful application of a grid search is that rather than using it for finding the global optima, a coarse grid search can instead be used to prune the search space for favorable regions, which can be used as initial guesses by other optimizers. Furthermore, since there are no random elements in the algorithm, it will always produce equal results with the same inputs, thus satisfying the criterion of repeatability.

A final advantage is that the user knows beforehand the inputs that the grid search will run through the cost function (these are the columns of the combinations matrix, e.g. in equation (13)), and therefore the user can choose to skip some, based on external criteria. For example, the user can impose a maximum total flight time, as in Table 1. Based on this, the user can eliminate some combinations before evaluating the function, which can save computation time.

5.2 Pattern Search

Pattern search is a very powerful built-in MATLAB optimizer, called “patternsearch.m” [20]. It is essentially an iterative adaptive grid search which is also capable of finding global minima. It requires an initial guess to start, and employs the following algorithm:

For a problem $\min F(\bar{x})$, an initial guess \bar{x}_0 and a grid size for every variable $\bar{\Delta}$ is defined. Then, the following iteration is performed. Note that the grid size for each variable will be used both as a positive step and a negative step.

1. Evaluate $F(\bar{x}_0)$
2. Evaluate $F(\bar{x}_0 + \bar{\Delta})$
3. If $F(\bar{x}_0 + \bar{\Delta}) < F(\bar{x}_0)$, set $\bar{x}_0 = \bar{x}_0 + \bar{\Delta}$, increase $\bar{\Delta}$
4. If $F(\bar{x}_0 + \bar{\Delta}) > F(\bar{x}_0)$, decrease $\bar{\Delta}$
5. If $\bar{\Delta} < tol$, stop, minimum is found. Else, repeat from step 1.

Note that this is a simplified version of the pseudocode; more detailed information is publicly available [20]. Also note that it is capable of handling all types of constraints.

5.2.1 Implementation within the program

Since pattern search relies on an initial guess, is to be used at least after another pre-optimizer (such as the grid search), which is to give it its best solution.

The tolerance for which to consider the problem converged is set to relatively high ($tol=10^{-4}$). This implies the program stops once the solutions are within an accuracy of 10^{-4} days (~9 seconds), or 100 km for DSM point. This is considered sufficient for a solution of the trajectory.

5.2.2 Notes on pattern search

Pattern search has the two major advantages needed at this stage: it is a semi-global optimizer, and it produces repeatable results, since there are no random elements. Being a standard MATLAB function it is also easily implemented, and, like discussed in Section 3: it has already been very efficiently programmed by experts in the field.

It has been found to be very suitable for the problems at hand. It is capable of moving through the search space reasonably well with low number of function evaluations, and since it does not contain derivative based decisions, it can easily deal with strong gradients associated with penalty functions. Both are important, since there are a lot of nonlinear constraints and many minima in the search space.

5.3 Genetic Algorithm

This paper will only outline the general principle of genetic algorithms, since this technique is well known in the optimization world, and many sources exist to learn more about this [21]. It is a heuristic global optimization method which evolves an initial population (a number of control vector combinations) through several generations (iterations), each time changing the population according to particular rules. In the case of genetic algorithms, the rule mimics natural selection, wherein members of the population are able to semi-randomly “reproduce” and yield new members of population which are combinations of the parents. Members who produce lower cost function values are given advantages, and others are eliminated. Other elements are introduced, like migration, mutation and crossover; this adds another element of randomness to the algorithm.

5.3.1 Implementation within the program

The MATLAB built-in genetic algorithm “ga.m” is used [22]. It is set up to take a predefined population from the best results of the grid search optimization. If the grid search cannot provide the initial population desired by the GA, the population size is adjusted to the number available.

It has been found that a high population, low generation algorithm tends to yield the best results (usually in the order of 200 members for 10-15 generations is sufficient). Since this algorithm also does not need to cycle through very many combinations, it can deal with relatively larger problems.

5.3.2 Notes on genetic algorithm

It has been found that the genetic algorithm is capable of exploring more regions of the search space that hadn't been previously discovered by grid search (due to poor resolution) or pattern search (due to poor starting condition). Thus it is capable of finding more solutions. However it does not yield repeatable results, which are sometimes critical.

Since it does not require an initial guess, it can be the only algorithm used in an optimization strategy. However, it has been found that even a very rough grid search to get a few points significantly helps the runs. Similar to the pattern search, it is capable of handling penalty function regions very well, since the strong gradients involved are not used by the algorithm.

The GA tends to be rather slow, which is typical of heuristic algorithms. However, since it is a built-in routine, it is robust and contains many customizable options which the user can choose to change depending on the problem [22]. It has also been observed that rather than using it to find the absolute global optima, a secondary use is to navigate the search space

better, looking for more favorable regions. Other optimizers can then take the best members of the population and use faster methods to converge.

5.4 Other Optimizers

It is worth noting that there are many other optimizers available. Due to the reasons mentioned in Section 3, only the ones pre-programmed by MATLAB have been investigated, and all are inferior to the optimizer's discussed in this paper. This might not always be the case for any optimization problem, as the performance of optimizers is often dependent on the problem at hand.

An unusual choice was that no gradient based methods have been used. This was a deliberate decision for a number of reasons. It was found that the cost function is extremely "jagged", and thus contains many local minima and maxima, which in turn poses a limit for any gradient based method. Furthermore, penalty functions produce very large gradients (in fact, since the cost function "changes" when a nonlinear constraint is violated, the gradient is 'infinite'). This causes many problems for gradient based methods, which rely on smooth functions. In the end, it was found that such methods could at best provide extremely modest improvements, at the expense of computation time. Hence they were eliminated entirely in favor of non-gradient based solvers.

Due to the modular structure of the code, further developers of the program will be able to easily add new optimization techniques, even outside the scope of MATLAB's built-in algorithms.

5.5 Final Optimization Strategy

Having described the optimizers to be used, the final step is to determine the order in which to use them. The following order has proven to be the best strategy.

Grid search – This is the starting optimizer. It has been found that even a coarse grid tends to help any further optimization attempt made. It is set as the starter, as it will sample the entire space evenly without any preference. However, due to the "curse of dimensionality", the grid search only optimizes the simplified problem, in order to achieve an acceptable grid resolution with shorter run times.

Genetic algorithm – This is the second optimizer in line, which the user can choose to deactivate. The algorithm will take the best N points from the grid search (to be determined by the user) as initial population (if there are fewer grid points than desired population, the population size is adjusted). This algorithm runs with the full problem, and takes the initial guess of DSM position in the middle of the unperturbed trajectory found by the grid search.

This algorithm has the advantage of being able to explore the search space better, and therefore it can find more local optima, however it does not yield repeatable results with equal inputs. Therefore, the user might want to deactivate it depending on what the program is used for. Generally, if one wants to perform sizing studies, repeatable results are necessary. The typical case is if the user wants to investigate the effect of changing a particular variable. In that case, the entire program needs to be run multiple times, each time with slightly different inputs. If the genetic algorithm is active, the user cannot tell whether the difference in results is due to the heuristic nature of the algorithm, or due to the different inputs. If on the other hand, the user wishes to find the absolute best point, it is useful to activate it.

Pattern search – This is the final optimization algorithm to be applied. It will use the best result from any previous optimizers as a starting point. It is rather fast in converging, and can

reach 'basin bottoms' rather quickly. The full problem is used with this algorithm. Due to its proven effectiveness with this type of functions, this optimizer is always left active. Even in the situation where it is not strictly necessary (because previous optimizers have already reached the global optimum) the pattern search does not slow down the program, as convergence will be much faster.

6. Results and Discussion

To validate the VISITOR tool, previously flown missions were used as test cases. The mission planetary sequence for each of these missions was input in VISITOR, along with ranges around the flown initial date and time-of-flights. The resulting optimal trajectory was then compared to the actual trajectory. The results of the analysis for seven flown interplanetary missions are shown in Section 6.1. Then, the results will be discussed in Section 6.2.

6.1 Case Analysis Results

To perform a preliminary evaluation of the performance of VISITOR, the mission sequence of a large number of flown missions were used. The selected missions are shown in Table 3, including which of the capabilities of VISITOR will be tested. Note that only missions with at least one GA maneuver were chosen, as direct trajectories do not allow for much variation. Also listed are in which leg(s) or encounter(s) these elements will occur. The bracketed numbers refer to asteroid and comet identification numbers.

Table 3: Summary of test case missions

Mission	Planet sequence	Planet ops	DSM	RGA	Multi-rev	Asteroid
Voyager 2 [23]	EJSUN	-	-	-	-	-
Galileo [11]	EVE(951)E(243)J	J – arrival	-	-	-	Flyby, flyby
Cassini [24]	EVVEJS	S – arrival	VV	-	-	-
NEAR Shoemaker [13]	E(253)E(433)(433)	-	(253)E	-	-	Flyby, rendezvous
Rosetta [6]	EEME(2867)E(21)(67P)	-	(21)(67P)	EE	EM	Flyby, flyby, rendezvous
New Horizons [25]	EJP	-	-	-	-	-
Juno [7] [26]	EEJ	J – arrival	EE	-	EE	-

It must be noted that strictly speaking Galileo flew an RGA trajectory between the two Earth GA maneuvers. However, as it performed a flyby of 951 Gaspra in this leg, the RGA capability of VISITOR will not be tested. The same holds for Rosetta, which visited 2867 Šteins during an RGA trajectory with Earth. In addition, the original trajectory for NEAR Shoemaker did not plan for two encounters with 433 Eros, but due to an engine failure, an extra leg was necessary to complete the mission [13].

The case analysis was performed in two ways: first, the exact encounter dates were input in VISITOR without allowing these to vary, in order to confirm that the actual trajectory could be reconstructed to a sufficient degree, this was done without optimizers. Second, bounds were increased and the optimization routines were used to find a solution with the same mission sequence. These two analyses will be discussed in the following subsections. Note that both analyses allow VISITOR to optimize for DSM position and timing, as it is not possible to fix these values in the user input.

6.1.1 Reproduction of Flown Trajectories

To reproduce the flown trajectories, the exact encounter dates were entered in VISITOR, and were not allowed to vary. If the mission used DSMs, the position and timing thereof were still allowed to be changed by the pattern search routine. No genetic algorithm was used for this analysis. As the computed trajectories have identical encounter dates to the flown trajectories, the computed excess velocity at Earth, DSM burn magnitudes (if applicable), and insertion burn magnitudes (if applicable) are compared to the actual values. The results of this analysis are shown in Table 4. Note that the computed DSM burn magnitudes include the GA burns that are affected by the DSM. This analysis provides benchmark values for the subsequent optimization analyses.

Table 4: Benchmark results for reproduction of flown trajectories

Mission	V_{∞} at Earth [km/s]		ΔV at DSM [km/s]		ΔV at insertion [km/s]	
	Actual	Computed	Actual	Computed	Actual	Computed
Voyager 2 [27]	10.119	10.128	-	-	-	-
Galileo [28] [11]	3.61	3.933	-	-	0.805 ^[1]	0.742
Cassini [24] [29]	4.254	4.043	0.466	0.451	0.613	0.587
NEAR Shoemaker [13]	5.089	4.896	0.269 ^[2]	0.489	0.010	0.794
			0.932 ^[2]	0.540		
Rosetta [6]	3.547	3.978	0.789 ^[2]	0.900	0.794	0.797
New Horizons [25]	12.806	12.587	-	-	-	-
Juno [7] [26]	5.550	5.536	0.776 ^[3]	0.759	? ^[4]	0.475

^[1] Value includes the effect of a GA maneuver around Io
^[2] Value does not include numerous small trajectory correction maneuvers (TCM's)
^[3] Combined value of two DSM's in quick succession
^[4] Juno has not yet arrived at Jupiter, value unknown

6.1.2 Optimization of Flown Mission Sequences

To test the optimization capabilities of VISITOR, the launch and encounter dates were given windows, within which these variables could be freely varied by the optimization routines. The bounds used consisted of the initial date ± 30 days, and the window size around the time-of-flight of each leg of the nominal trajectory dependent on the target: ± 30 days was used for the inner planets and most asteroids, and ± 100 days was used for the outer planets and 67P. The progressively larger windows allow larger angular variations of bodies which have longer orbits.

For each case, the same optimization strategy will be used. A relatively quick grid search will generate the 200 best combinations, which will be used as the initial population for a genetic algorithm run. Three grid points per variable will be used in the case of missions with more than four legs, and five grid points per variable will be used in the other cases. The genetic algorithm will then run with a population of 200 individuals for 50 generations, to allow decent convergence while avoiding excessive run times. The best result from the genetic algorithm is then fed into pattern search to obtain a final solution, with a limit set of 1000 function evaluations.

The results of this analysis for the seven test cases can be seen in Table 5. As with Table 4, the excess velocity at Earth, DSM (plus corresponding GA's) burn magnitudes, and insertion burns will be compared, along with total mission ΔV . In this comparison, the computed results from Table 4 are treated as the "nominal" trajectory. In addition, the mean of the absolute value

of the difference between encounter dates is included per mission, to provide an indication of how close the optimized result is to the nominal result. Also shown is the runtime of the code, performed on an Intel® Core™ i5-2520M 2.50 GHz CPU with 4.00 GB of RAM. Note that MATLAB will only use 25% of the CPU per core at any given time. In this case, only one core is used, as no parallel processing capability has yet been added.

For comparison, Table 6 contains the results for identical runs, but without the genetic algorithm such that repeatable results are obtained. Thus, the single best result from the grid search will be used as a starting point for pattern search, a technique designated by GSPS. These results are compared to those which include the genetic algorithm, treating the optimized results as the new nominal trajectory. Thus, the difference between the encounter dates is also measured with respect to the optimized solution.

Note that all evaluations assume a 300 km altitude circular parking orbit around the Earth as an initial orbit, for computing total mission ΔV . This was chosen as it is a good approximation of actual launch practices, and since more accurate data was not available.

Table 5: Results of full optimization compared to the nominal trajectory

Mission	Runtime [s]	Mean Δ date [days]	Total mission ΔV [km/s]		V_{∞} at Earth [km/s]		ΔV at DSM [km/s]		ΔV at insertion [km/s]	
			Nominal	Optimized	Nominal	Optimized	Nominal	Optimized	Nominal	Optimized
Voyager 2	813.4	59.2	7.255	6.691	10.128	9.406	-	-	-	-
Galileo	682	9.3	5.279	4.682	3.933	3.866	-	-	0.742	0.721
Cassini	409.2	3.2	5.124	5.346	4.043	3.890	0.451	0.883	0.587	0.591
NEAR Shoemaker	375.3	24.6	6.071	7.122	4.896	4.938	0.489	1.591	0.794	0.789
							0.540	0.478		
Rosetta	13,442.1	22.9	6.086	5.560	3.978	3.793	0.900	0.087	0.797	0.744
New Horizons	142.9	38	8.970	9.023	12.587	12.703	-	-	-	-
Juno	123.5	2.7	5.756	5.688	5.536	5.676	0.759	0.663	0.475	0.438

Table 6: Results of the GSPS method compared to the results of the full optimization

Mission	Runtime [s]	Mean Δ date [days]	Total mission ΔV [km/s]		V_{∞} at Earth [km/s]		ΔV at DSM [km/s]		ΔV at insertion [km/s]	
			Optimized	GSPS	Optimized	GSPS	Optimized	GSPS	Optimized	GSPS
Voyager 2	256.8	0.2	6.691	6.691	9.406	9.406	-	-	-	-
Galileo	137.3	3.4	4.682	5.365	3.866	3.933	-	-	0.721	0.724
Cassini	104.4	26.6	5.346	5.184	3.890	2.947	0.883	1.025	0.591	0.553
NEAR Shoemaker	100.7	5	7.122	7.285	4.938	4.853	1.591	1.924	0.789	0.729
							0.478	0.403		
Rosetta	3,873.5	3.4	5.560	6.541	3.793	3.902	0.087	0.614	0.744	0.665
New Horizons	10.4	0.7	9.023	9.035	12.703	12.710	-	-	-	-
Juno	18.1	33	5.688	7.169	5.676	5.715	0.663	2.126	0.438	0.439

The average ΔV offset from the nominal result to the optimized and GSPS results across all missions was 8.2%. For the optimized results, this value is slightly lower, 7.3%, and the GSPS solutions have a slightly higher average offset of 9.1%. The average increase in run time when

using the full optimization rather than the GSPS technique is a factor 5.7. Note that in a few cases, particularly Juno, the GSPS solution is markedly worse than the optimized solution.

6.2 Discussion

From the results shown in Section 6.1, a number of differences can be noted. The first part of the discussion will be devoted to the reproduction of the flown trajectories, and the second part will relate to the optimization process.

6.2.1 Discussion on Trajectory Reproduction

Based on the results from Table 4, VISITOR is able to relatively accurately reproduce most trajectories, with the notable exception of NEAR Shoemaker. Particularly with respect to the insertion burn, the difference is very significant, and while the DSM burns have the correct order of magnitude, the computed values show major discrepancies with the actual burns.

These large errors can have a number of different causes. First, the trajectory flown by NEAR Shoemaker has numerous planned TCM's [13], which cannot be simulated by VISITOR. While each of these maneuvers is small, their added effect can have a significant influence on the orbit.

Second, and perhaps most significantly, NEAR Shoemaker was never intended to first fly by 433 Eros before waiting more than a year to actually rendezvous with the asteroid [13]. Originally, the first encounter with 433 Eros would have been the orbit insertion. However, due to an engine misfire, NEAR Shoemaker was not able to perform this maneuver, and the extra revolution around the Sun and eventual rendezvous was implemented to salvage the mission. This could explain the large discrepancy between the magnitudes of the actual and computed second DSM burn, as this burn would have been suboptimal. However, when combined with the ΔV required for orbit insertion, the total expenditure of this last phase of the trajectory of the real mission is still less than computed by VISITOR.

To explain the large difference in insertion ΔV , it is possible be that after the second DSM, NEAR Shoemaker remained close enough to 433 Eros to be influenced by the latter's gravity, as the DSM reduced the relative velocity to near-zero [13]. Again, this is something that VISITOR is unable to simulate, as it only uses the patched conic approximation.

Apart from the large discrepancies when discussing NEAR Shoemaker, the other missions examined show good result reproduction, matching all real values to within a few hundred m/s. This shows that VISITOR is able to reasonably accurately reproduce the results of flown missions, which validates the tool for high-level sizing purposes.

6.2.2 Case Discussion on Trajectory Optimization

A number of remarks can be made with regards to the trajectory optimization performance of VISITOR. First, the full optimization sequence will be considered, which includes the genetic algorithm pre-optimization. The most important remark to make is that, as with all heuristic methods, genetic algorithms incorporate an element of randomness [21], and can thus have a significant impact on the solution to the problem, especially one as irregular as interplanetary trajectory optimization. Ideally, if ran for a very long time (thousands of individuals for hundreds of generations), the solution should converge to the global optimum, but there is no guarantee of this.

With this in mind, the results from Table 5 and Table 6 can be examined. Each mission will be discussed individually below. A general discussion of the performance of VISITOR's trajectory optimization will be done in Section 6.2.3.

Voyager 2 – The optimized solution for Voyager 2 shows some improvement over the nominal case, with respect to reduction in excess velocity and total cost function. The reason for this is simply due to the added windows around the time of flights, and VISITOR makes liberal use of this: The launch date is delayed by 12 days, with the subsequent Jupiter, Saturn, Uranus, and Neptune encounters occurring 24, 50, 87, and 123 days later than nominal, respectively. In reality, Voyager 2 was most likely subject to launch constraints, as Voyager 1 was to be launched 12 days after Voyager 2 in order to reach Titan [30].

As a result of the relatively simple, continuously outwards trajectory of Voyager 2, turning off the genetic algorithm does not change the result significantly, only delaying the launch by an extra day. However, it does significantly reduce run time of the code, as expected, a trend which will be seen throughout these cases.

Galileo – The optimized solution for Galileo also shows some improvement over the nominal trajectory with respect to total mission ΔV . The main difference occurs in the final mission leg from 243 Ida to Jupiter, which takes 53 days longer than the nominal result. For the other encounters, the maximum deviation from the nominal result is 3 days. The result of the longer final mission leg is a better flyby geometry of 243 Ida, resulting in a reduction in flyby ΔV by more than 200 m/s. The slight variations in the other dates also reduce flyby ΔV 's at the other encounters. It is possible that the final leg of Galileo's mission was subject to additional constraints, necessitating it to arrive at Jupiter earlier. Also, the slight variations in the other dates can be explained by the errors introduced by the patched conic approximation, resulting in a slightly different trajectory being optimal.

However, when switching off the genetic algorithm, the solution becomes markedly worse, requiring more total mission ΔV than the nominal case. While the excess velocity and insertion ΔV are good matches for the optimized solution, the GA geometry is not as good when only using GSPS, resulting in more ΔV being expended at flybys. It is possible that the optimum solution lies in a very narrow range, requiring the better search capability of a genetic algorithm.

Cassini – The optimized solution for Cassini is slightly worse in terms of total mission ΔV than the nominal one, mostly resulting from a larger DSM ΔV . For the rest, the encounter dates are a very close match for the nominal trajectory. The fact that the DSM is suboptimal can be contributed to the fact that the genetic algorithm was not able to properly reproduce its positioning and timing.

However, the GSPS solution actually performs better than the optimized solution. While this seems counter-intuitive, it is most likely a result of the inherent random component of the genetic algorithm: it could be possible that the genetic algorithm is "stuck" in a wide local optimum, from which pattern search is then unable to "escape". The GSPS solution also shows quite a large difference in encounter dates with respect to the optimized solution: both the departure and arrival dates are significantly delayed, by 33 and 84 days respectively, while the other dates are fairly close to the optimized solution. The DSM performance is still a bit inaccurate.

NEAR Shoemaker – The optimized solution for NEAR Shoemaker is also slightly worse than nominal in terms of total mission ΔV . As with Cassini, most of this difference is accounted for by the first DSM, which expends more than 1 km/s of ΔV more than the nominal case. A probable cause is the large variations in encounter dates with respect to the nominal solution: while the optimized departure date is 15 days earlier than nominal, the final arrival date is 55 days later than nominal.

The GSPS solution has similar performance to the optimized solution, with an average deviation of 5 days at each encounter. Total mission ΔV values are also very similar, implying that the nominal solution lies within a very narrow range of the search space.

Rosetta – The optimized solution for Rosetta is a bit better than the nominal solution, despite it being the most complex mission analyzed in terms of capabilities tested. The main source of the improvement in total mission ΔV is the reduction of the DSM burn by more than 800 m/s, which in turn is caused by the large differences in encounter dates: The optimized solution departs 30 days before and arrives 87 days after the nominal solution. As with Galileo and Voyager, Rosetta was likely subject to similar launch or mission-related constraints which are not taken into account here. Also note the long run time, which is caused by the analysis of the DGRA trajectory flown between launch and the first flyby.

When analyzing the GSPS results, a worse result than both the nominal and optimized cases is observed. The encounter dates are close to the optimized trajectory, except for the arrival date which has been pushed back by 12 days. The result of this is that the DSM ΔV is once again significantly larger.

New Horizons – The optimized solution for New Horizons is very similar to the nominal case, with the largest difference being the arrival date, which is 109 days earlier than the nominal case. The GSPS solution reflects this, being almost exactly the same as the optimized case. While 109 days difference seems significant, the target of this leg is Pluto, which moves a very small amount in this length of time. Therefore, the total cost function will not change much over this range.

Juno – The optimized result for Juno shows a slight improvement over the nominal case, caused by smaller DSM and insertion ΔV 's. The encounter dates are also very close to the nominal solution. However, the GSPS solution is significantly worse, primarily due to a much higher DSM ΔV . The likely cause is that the best point from the grid solution does not allow pattern search to “escape” from that local minimum, while the genetic algorithm can more easily cover a larger region of the search space.

6.2.3 General Discussion on Trajectory Optimization

A number of trends can be discerned based on the results obtained. First, it is clear that the function describing interplanetary trajectories is highly irregular, as it is very rare for two different methods to converge to the same minimum. Even if the trajectory is only a few days from the nominal result, as with Cassini, the total mission ΔV will still be quite different. While not unexpected, this does highlight the challenges of finding good interplanetary trajectories.

Second, in general, the use of a genetic algorithm in the optimization scheme can improve the total mission ΔV , although it is possible that the convergence is to a suboptimal solution, as with Cassini and NEAR Shoemaker. As such, there is a certain element of luck involved, dependent on the fineness of the initial grid search and the amount of generations and initial population in the genetic algorithm. However, given enough time, heuristic methods will in general converge in a stable manner, and for this reason such methods are often used in

solving interplanetary trajectory problems [1]. A disadvantage of this is that it is difficult to obtain repeatability without excessively long run times.

Third, it is apparent that if the absolute global optimum is desired, the GSPS method is not well suited for the task. The main disadvantage lies in the fact that pattern search is only given a single initial point, and while it can fairly effectively examine the local search space, it is not capable of covering the entire search space. Thus, if the grid search returns a result which is in the wrong area of the search space, it is very difficult for pattern search to converge to the global optimum with a very irregular function.

However, the GSPS method is repeatable: the same inputs will always yield the same outputs. Also, the grids used in the sample cases were relatively coarse (3 or 5 points per variable), so increasing the grid fineness might improve the solution. Finally, the simpler the trajectory, such as Voyager 2 or New Horizons, the more regular the cost function, and therefore pattern search is more easily able to find the “global” minimum.

Overall it can be said that the optimizers are generally able to find close trajectories to the nominal. Note also that computation times were purposely kept as low as possible to allow VISITOR to serve as a proper computation tool. For example, reproducing Cassini with a FORTRAN genetic algorithm to high fidelity can take several hours [31], whereas it took VISITOR a little under 7 minutes. Thus the goal of obtaining fast results for fast sizing purposes has also been achieved.

7. Conclusions

The VISITOR tool was developed to solve the impulsive interplanetary trajectory problem. For a given mission sequence, it uses a multiple gravity assist model based on the patched conic approximation, with the ability to analyze deep space maneuvers, asteroid encounters, resonant gravity assists, and a number of different types of planetary operations based on real planet orientations. The cost function can then be formulated in terms of excess velocity, burn ΔV , or initial stack mass for a given final payload. This cost function is then minimized using a hybrid optimization approach, consisting of an initial coarse grid search over a simplified problem formulation, an optional genetic algorithm pre-optimization over the full problem, and a final optimization using pattern search over the full problem.

To validate the results produced by VISITOR, seven flown interplanetary missions were used as test cases, being Voyager 2, Galileo, Cassini, NEAR Shoemaker, Rosetta, New Horizons, and Juno. First, benchmark values were produced by fixing the encounter dates of these missions in VISITOR and comparing the results to the actual missions. Then, two optimization strategies were compared: a full optimization using the genetic algorithm pre-optimization, and a fast optimization which did not employ the genetic algorithm. The average offset between the benchmark values and the optimized results in total mission ΔV was 8.2%. The full optimization achieved lower values than the fast optimization, 7.3% as opposed to 9.1%, at the cost of longer run times by an average factor of 5.7. These results prove that VISITOR is able to find solutions with realistic values for total mission ΔV .

A number of recommendations for future VISITOR development can be made, covering the areas of modeling and optimization. With respect to modeling, the most important recommendation is the inclusion of the ability to analyze low-thrust MGA trajectories. Also, the inclusion of more detailed planetary operation analysis, such as the simulation of large planetary moons, aerocapture, EDL, ascent analysis, and spacecraft rendezvous, would result in a more realistic simulation. Finally, more intricate mass models than the simple iterative method presented here could also be implemented.

With respect to optimization, new optimization strategies should be investigated, along with fine-tuning the parameters of each implemented method. Through the inclusion of more

advanced heuristic methods, such as evolutionary branching or monotonic basin hopping, the overall global optimization performance could be improved.

As a final point, it should be mentioned that it would be more appropriate to validate the performance of VISITOR with cases also using an externally-developed simplified model, rather than flown missions which can be subject to other constraints than cannot be considered by VISITOR.

Bibliography

- 1] D. Izzo and T. Vinko, "ACT / ESA - Informatics and Applied Mathematics - GTO
Database," ESA, [Online]. Available: <http://www.esa.int/gsp/ACT/inf/projects/gtop/gtop.html>.
[Accessed 16 May 2014].
- 2] "SPICE," NASA, 31 3 2014. [Online]. Available: <http://naif.jpl.nasa.gov/naif/>. [Accessed
5 5 2014].
- 3] "Solar System Dynamics," NASA - Jet Propulsion Laboratory, [Online]. Available:
<http://ssd.jpl.nasa.gov/?ephemerides>. [Accessed 5 5 2014].
- 4] Vallado, *Fundamentals of Astrodynamics and Applications*, El Segundo, CA: Microcosm
Press & Kluwer Academic Publishers, 1999.
- 5] R. H. Gooding, "A procedure for the solution of Lambert's orbital boundary-value
problem," *Celestial Mechanics and Dynamical Astronomy*, p. 48:145, 1990.
- 6] J. Schoenmaekers and R. Bauske, "Re-Design of the Rosetta Mission For Launch in
2004," in *Proceedings of the 18th International Symposium on Space Flight Dynamics*,
Munich, Germany, 2004.
- 7] T. D. Kowalkowski, J. R. Johannesen and T. Lam, "Launch Period Development for the
Juno Mission to Jupiter," in *AIAA/AAS Astrodynamics Specialist Conference and Exhibit*,
Honolulu, HI, 2008.
- 8] J. Englander, "Automated Trajectory Planning for Multiple-flyby Interplanetary
Missions," University of Illinois, Urbana, 2013.
- 9] D. F. Landau, J. M. Longuski and P. A. Penzo, "Method for Parking-Orbit Reorientation
for Human Missions to Mars," *Journal of Spacecraft and Rockets*, vol. 42, no. 3, pp. 517-
522, 2005.
- 10] L. P. Gefert and K. J. Hack, "Low-Thrust Control Law Development for Transfer from
Low Earth Orbits to High Energy Elliptical Parking Orbits," in *AAS/AIAA Astrodynamics
Specialist Conference*, Girdwood, AK, 1999.
- 11] L. A. D'Amario, L. E. Bright and A. A. Wolf, "Galileo Trajectory Design," *Space Science
Reviews*, vol. 60, no. 1-4, pp. 23-78, 1992.
- 12] J. V. McAdams, D. W. Dunham, R. W. Farquhar, A. H. Taylor and B. G. Williams,
"Trajectory Design and Maneuver Strategy for the MESSENGER Mission to Mercury,"
Journal of Spacecraft and Rockets, vol. 43, no. 5, pp. 1054-1064, 2006.
- 13] D. M. Dunham, J. V. McAdams and R. W. Farquhar, "NEAR Mission Design," *John
Hopkins APL Technical Digest*, vol. 23, no. 1, pp. 18-33, 2002.
- 14] JPL SSD Group, "Asteroid & Comet SPK File Generation Request," Jet Propulsion
Laboratory, [Online]. Available: <http://ssd.jpl.nasa.gov/x/spk.html>. [Accessed 18 March
2014].
- 15] D. F. Rico, H. H. Sayani and R. F. Field, "History of Computers, Electronic Commerce
and Agile Methods," in *Advances in Computers*, Elsevier Science Publishing Co Inc, 2014,
pp. Volume 73, pages 1-55.
- 16] MathWorks, "Quickly convert MATLAB code to C with MATLAB Coder.," MathWorks,
[Online]. Available: [http://www.mathworks.com/programs/nrd/matlab-convert-to-c-trial-
request.html?ref=ggl&s_eid=ppc_2790](http://www.mathworks.com/programs/nrd/matlab-convert-to-c-trial-request.html?ref=ggl&s_eid=ppc_2790). [Accessed 15 05 2014].
- 17] A. E. Smith and D. W. Coit, "Penalty Functions," Oxford University Press and Institute of
Physics Publishing, Oxford, 1996.

- 18] | J. Pintér, "Global Optimization," MathWorld--A Wolfram Web Resource, [Online]. Available: <http://mathworld.wolfram.com/GlobalOptimization.html>. [Accessed 13 05 2014].
- 19] | R. E. Bellman, Dynamic programming, Princeton: Princeton University Press, 1957.
- 20] | MathWorks, "Direct Search," MathWorks, [Online]. Available: <http://www.mathworks.com/help/gads/direct-search.html>. [Accessed 14 05 2014].
- 21] | Y. Davidor, H. Schwefel and R. Männer, Genetic algorithms with multi-parent recombination, Springer, 1994.
- 22] | MathWorks, "Genetic Algorithm," [Online]. Available: <http://www.mathworks.com/help/gads/genetic-algorithm.html>. [Accessed 14 05 2014].
- 23] | R. P. Rudd, J. C. Hall and G. L. Spradlin, "The Voyager Interstellar Mission," *Acta Astronautica*, vol. 40, no. 2-8, pp. 383-396, 1997.
- 24] | F. Peralta and S. Flanagan, "Cassini Interplanetary Trajectory Design," *Control Engineering Practice*, vol. 3, no. 11, pp. 1603-1610, 1995.
- 25] | Y. Guo and R. W. Farquhar, "New Horizons Mission Design," *Space Science Reviews*, vol. 140, no. 1-4, pp. 49-74, 2008.
- 26] | T. Greicius and B. Dunbar, "NASA - Juno Spacecraft Cruise Trajectory," NASA, 28 July 2011. [Online]. Available: http://www.nasa.gov/mission_pages/juno/multimedia/Juno20110727-3.html. [Accessed 14 May 2014].
- 27] | R. L. Heacock, "The Voyager Spacecraft," in *James Watt International Gold Medal Lecture*, London, UK, 1980.
- 28] | H. F. Meissinger, S. Dawson and J. R. Wertz, "A Low-Cost Modified Launch Mode for High-C~ 3 Interplanetary Missions," *Advances in the Astronautical Sciences*, vol. 97, pp. 1693-1708, 1998.
- 29] | A. Wessen, K. Munsell, E. Piazza and A. Yu, "Cassini Solstice Mission: Saturn Arrival -- A Guide to Saturn Orbit Insertion," NASA, [Online]. Available: <http://saturn.jpl.nasa.gov/photos/imagetails/index.cfm?imageId=794>. [Accessed 15 May 2014].
- 30] | C. E. Kohlhase and P. A. Penzo, "Voyager Mission Description," *Space Science Reviews*, vol. 21, no. 2, pp. 77-101, 1977.
- 31] | B. K. B. W. Sam Wagner, "GPU Accelerated Genetic Algorithm for Multiple Gravity-Assist and Impulsive dV Maneuvers," in *AIAA/AAS Astrodynamics Specialist Conference*, Minneapolis, Minnesota, 2012.
- 32] | D. Eagle, "Modeling Aero-assist Flight Mechanics with MATLAB - File Exchange - MATLAB Central," The MathWorks, Inc., 19 August 2013. [Online]. Available: <http://www.mathworks.com/matlabcentral/fileexchange/43121-modeling-aero-assist-flight-mechanics-with-matlab>. [Accessed 19 May 2014].

Appendix

Here the full results from the validation cases are shown. This is the raw data obtained from VISITOR. For each of the seven missions analyzed, three tables will be shown: the first shows the nominal case where the dates were hard coded into the program, then the case where the genetic algorithm was not used, and lastly the case where the genetic algorithm is used.

NEAR-Showmaker:

MISSION SUMMARY - E1E22 1996 opportunity

BODY	EVENT	Date	MET	TOF	vinfm-	vinfm+	Deltav	Ventry	AltFB	Altp,i	Alta,i	I,i	Altp,f	Alta,f	I,f
Earth	Departure	17-Feb-1996	0.00	0.00	0.0000	4.8958	0.0000	0.0000	0.0	0.0	0.0	0.0	0.0	0.0	0.0
Earth	- Heliocentric injection	17-Feb-1996	0.00	0.00	0.0000	0.0000	4.2469	0.0000	0.0	300.0	300.0	16.4	300.0	0.0	16.4
Asteroid 1	Swingby	27-Jun-1997	496.00	496.00	9.8426	10.1029	0.4508	0.0000	0.0	0.0	0.0	0.0	0.0	0.0	0.0
n/a	DSM	10-Oct-1997	601.00	105.00	0.0000	0.0000	0.0000	0.0000	0.0	0.0	0.0	0.0	0.0	0.0	0.0
Earth	Swingby	23-Jan-1998	706.00	105.00	6.7257	6.7963	0.0383	0.0000	901.0	0.0	0.0	0.0	0.0	0.0	0.0
Asteroid 2	Swingby	23-Dec-1998	1040.00	334.00	0.9539	0.9539	0.0000	0.0000	0.0	0.0	0.0	0.0	0.0	0.0	0.0
n/a	DSM	27-Jul-1999	1256.00	216.00	0.0000	0.0000	0.5403	0.0000	0.0	0.0	0.0	0.0	0.0	0.0	0.0
Asteroid 2	Rendezvous Arrival	14-Feb-2000	1458.00	202.00	0.7944	0.0000	0.7944	0.0000	0.0	0.0	0.0	0.0	0.0	0.0	0.0
Total			1458.00 18.3167 22.7489 6.0707												

Best objective
6.0707

MISSION SUMMARY - E1E22 1996 opportunity

BODY	EVENT	Date	MET	TOF	vinfm-	vinfm+	Deltav	Ventry	AltFB	Altp,i	Alta,i	I,i	Altp,f	Alta,f	I,f
Earth	Departure	17-Feb-1996	0.00	0.00	0.0000	4.8533	0.0000	0.0000	0.0	0.0	0.0	0.0	0.0	0.0	0.0
Earth	- Heliocentric injection	17-Feb-1996	0.00	0.00	0.0000	0.0000	4.2296	0.0000	0.0	300.0	300.0	29.9	300.0	0.0	29.9
Asteroid 1	Swingby	01-Jun-1997	470.00	470.00	9.3499	8.4315	1.5907	0.0000	0.0	0.0	0.0	0.0	0.0	0.0	0.0
n/a	DSM	26-Sep-1997	587.13	117.13	0.0000	0.0000	0.0114	0.0000	0.0	0.0	0.0	0.0	0.0	0.0	0.0
Earth	Swingby	23-Jan-1998	706.19	119.06	6.3966	6.9523	0.3216	0.0000	2632.8	0.0	0.0	0.0	0.0	0.0	0.0
Asteroid 2	Swingby	18-Jan-1999	1066.19	360.00	0.8909	0.8855	0.0094	0.0000	0.0	0.0	0.0	0.0	0.0	0.0	0.0
n/a	DSM	24-Aug-1999	1284.19	218.00	0.0000	0.0000	0.3932	0.0000	0.0	0.0	0.0	0.0	0.0	0.0	0.0
Asteroid 2	Rendezvous Arrival	12-Apr-2000	1516.19	232.00	0.7286	0.0000	0.7286	0.0000	0.0	0.0	0.0	0.0	0.0	0.0	0.0
Total			1516.19 17.3660 21.1226 7.2845												

Best objective
7.2845

MISSION SUMMARY - E1E22 1996 opportunity

BODY	EVENT	Date	MET	TOF	vinfm-	vinfm+	Deltav	Ventry	AltFB	Altp,i	Alta,i	I,i	Altp,f	Alta,f	I,f
Earth	Departure	02-Feb-1996	0.00	0.00	0.0000	4.9378	0.0000	0.0000	0.0	0.0	0.0	0.0	0.0	0.0	0.0
Earth	- Heliocentric injection	02-Feb-1996	0.00	0.00	0.0000	0.0000	4.2641	0.0000	0.0	300.0	300.0	29.2	300.0	0.0	29.2
Asteroid 1	Swingby	31-May-1997	484.11	484.11	9.3188	8.4004	1.5907	0.0000	0.0	0.0	0.0	0.0	0.0	0.0	0.0
n/a	DSM	26-Sep-1997	602.18	118.07	0.0000	0.0000	0.0005	0.0000	0.0	0.0	0.0	0.0	0.0	0.0	0.0
Earth	Swingby	20-Jan-1998	718.98	116.80	6.6567	6.6567	0.0000	0.0000	3395.6	0.0	0.0	0.0	0.0	0.0	0.0
Asteroid 2	Swingby	15-Jan-1999	1078.06	359.08	0.9876	0.9876	0.0000	0.0000	0.0	0.0	0.0	0.0	0.0	0.0	0.0
n/a	DSM	24-Aug-1999	1299.06	221.00	0.0000	0.0000	0.4780	0.0000	0.0	0.0	0.0	0.0	0.0	0.0	0.0
Asteroid 2	Rendezvous Arrival	09-Apr-2000	1528.06	229.00	0.7886	0.0000	0.7886	0.0000	0.0	0.0	0.0	0.0	0.0	0.0	0.0
Total			1528.06 17.7517 20.9825 7.1220												

Best objective
7.1220

Juno:

MISSION SUMMARY - EEJ 2011 Opportunity

BODY	EVENT	Date	MET	TOF	Vinfm-	Vinfm+	DeltaV	Ventry	AltFB	Altp,i	Alta,i	I,i	Altp,f	Alta,f	I,f
Earth	Departure	06-Aug-2011	0.00	0.00	0.0000	5.5363	0.0000	0.0000	0.0	0.0	0.0	0.0	0.0	0.0	0.0
Earth	- Helio centric injection	06-Aug-2011	0.00	0.00	0.0000	0.0000	4.5227	0.0000	0.0	300.0	300.0	19.1	300.0	0.0	19.1
n/a	DSM	08-Nov-2012	460.80	460.80	0.0000	0.0000	0.7588	0.0000	0.0	0.0	0.0	0.0	0.0	0.0	0.0
Earth	Swingby	10-Oct-2013	796.06	33.29	10.4470	10.4470	0.0000	0.0000	1241.2	0.0	0.0	0.0	0.0	0.0	0.0
Jupiter	Target orbit insertion	06-Jul-2016	1796.00	1000.00	0.0000	0.0000	0.4747	0.0000	0.0	5000.0	0.0	7.3	5000.0	10000000.0	7.3
Jupiter	Arrival	06-Jul-2016	1796.00	0.00	5.4492	0.0000	0.0000	0.0000	0.0	0.0	0.0	0.0	0.0	0.0	0.0
Total															
Total										1796.00	15.8961	15.9833	5.7562		

Best objective
5.7562

MISSION SUMMARY - EEME2E31 2004 opportunity

BODY	EVENT	Date	MET	TOF	Vinfm-	Vinfm+	DeltaV	Ventry	AltFB	Altp,i	Alta,i	I,i	Altp,f	Alta,f	I,f
Earth	Departure	01-Feb-2004	0.00	0.00	0.0000	3.9017	0.0000	0.0000	0.0	0.0	0.0	0.0	0.0	0.0	0.0
Earth	- Helio centric injection	01-Feb-2004	0.00	0.00	0.0000	0.0000	3.8759	0.0000	0.0	300.0	300.0	4.3	300.0	0.0	4.3
Earth	Double hit	31-Jan-2005	365.26	365.26	3.9017	3.9063	0.0016	0.0000	1047.5	0.0	0.0	0.0	0.0	0.0	0.0
Mars	Swingby	30-Jan-2007	1094.26	729.00	8.6385	8.4384	0.1809	0.0000	1853.7	0.0	0.0	0.0	0.0	0.0	0.0
Earth	Swingby	12-Nov-2007	1380.26	286.00	8.1955	9.3396	0.9148	0.0000	12056.4	0.0	0.0	0.0	0.0	0.0	0.0
Asteroid 2	Swingby	07-Sep-2008	1680.26	300.00	8.5128	8.6784	0.2869	0.0000	0.0	0.0	0.0	0.0	0.0	0.0	0.0
Earth	Swingby	11-Nov-2009	2110.26	430.00	9.5815	9.5839	0.0017	0.0000	2696.0	0.0	0.0	0.0	0.0	0.0	0.0
Asteroid 3	Swingby	09-Jul-2010	2350.26	240.00	15.0487	15.0132	0.0615	0.0000	0.0	0.0	0.0	0.0	0.0	0.0	0.0
n/a	DSM	30-Aug-2012	3133.26	783.00	0.0000	0.0000	0.5527	0.0000	0.0	0.0	0.0	0.0	0.0	0.0	0.0
Asteroid 1	Rendezvous Arrival	27-Aug-2014	3860.26	727.00	0.6645	0.0000	0.6645	0.0000	0.0	0.0	0.0	0.0	0.0	0.0	0.0
Total															
Total										3860.26	54.5432	58.8615	6.5406		

Best objective
6.5406

MISSION SUMMARY - EEME2E31 2004 opportunity

BODY	EVENT	Date	MET	TOF	Vinfm-	Vinfm+	DeltaV	Ventry	AltFB	Altp,i	Alta,i	I,i	Altp,f	Alta,f	I,f
Earth	Departure	01-Feb-2004	0.00	0.00	0.0000	3.7931	0.0000	0.0000	0.0	0.0	0.0	0.0	0.0	0.0	0.0
Earth	- Helio centric injection	01-Feb-2004	0.00	0.00	0.0000	0.0000	3.8398	0.0000	0.0	300.0	300.0	70.1	300.0	0.0	70.1
Earth	Double hit	01-Feb-2005	365.26	365.26	3.7931	3.7963	0.0011	0.0000	1633.7	0.0	0.0	0.0	0.0	0.0	0.0
Mars	Swingby	27-Jan-2007	1090.88	725.63	8.5148	8.5650	0.0457	0.0000	2250.1	0.0	0.0	0.0	0.0	0.0	0.0
Earth	Swingby	08-Nov-2007	1376.13	285.25	8.4410	9.3988	0.7841	0.0000	14022.0	0.0	0.0	0.0	0.0	0.0	0.0
Asteroid 2	Swingby	04-Sep-2008	1676.63	300.50	8.6465	8.6455	0.0017	0.0000	0.0	0.0	0.0	0.0	0.0	0.0	0.0
Earth	Swingby	12-Nov-2009	2110.63	434.00	9.4265	9.3470	0.0564	0.0000	2810.6	0.0	0.0	0.0	0.0	0.0	0.0
Asteroid 3	Swingby	12-Jul-2010	2352.69	242.06	14.7596	14.7596	0.0000	0.0000	0.0	0.0	0.0	0.0	0.0	0.0	0.0
n/a	DSM	28-Jul-2012	3099.69	747.00	0.0000	0.0000	0.0866	0.0000	0.0	0.0	0.0	0.0	0.0	0.0	0.0
Asteroid 1	Rendezvous Arrival	15-Aug-2014	3848.19	748.50	0.7441	0.0000	0.7441	0.0000	0.0	0.0	0.0	0.0	0.0	0.0	0.0
Total															
Total										3848.19	54.3256	58.3052	5.5596		

Best objective
5.5596

Rosetta

MISSION SUMMARY - EEME2E31 2004 opportunity

BODY	EVENT	Date	MET	TOF	Vinfm-	Vinfm+	DeltaV	Ventry	AltFB	Altp,i	Alta,i	I,i	Altp,f	Alta,f	I,f
Earth	Departure	02-Mar-2004	0.00	0.00	0.0000	3.9781	0.0000	0.0000	0.0	0.0	0.0	0.0	0.0	0.0	0.0
Earth	- Helio centric injection	02-Mar-2004	0.00	0.00	0.0000	0.0000	3.9018	0.0000	0.0	300.0	300.0	67.1	300.0	0.0	67.1
Earth	Double hit	02-Mar-2005	365.26	365.26	3.9781	3.9864	0.0029	0.0000	614.9	0.0	0.0	0.0	0.0	0.0	0.0
Mars	Swingby	23-Feb-2007	1088.26	723.00	8.9651	8.8932	0.0630	0.0000	103.3	0.0	0.0	0.0	0.0	0.0	0.0
Earth	Swingby	11-Nov-2007	1349.26	261.00	9.6043	9.3900	0.1652	0.0000	6582.9	0.0	0.0	0.0	0.0	0.0	0.0
Asteroid 2	Swingby	05-Sep-2008	1646.26	437.00	8.7573	9.6839	1.0022	0.0000	0.0	0.0	0.0	0.0	0.0	0.0	0.0
Earth	Swingby	11-Nov-2009	2080.26	434.00	9.4234	9.6392	0.1558	0.0000	3189.2	0.0	0.0	0.0	0.0	0.0	0.0
Asteroid 3	Swingby	08-Jul-2010	2319.26	239.00	15.1529	14.8750	0.4813	0.0000	0.0	0.0	0.0	0.0	0.0	0.0	0.0
n/a	DSM	27-Jun-2012	3039.26	720.00	0.0000	0.0000	0.4190	0.0000	0.0	0.0	0.0	0.0	0.0	0.0	0.0
Asteroid 1	Rendezvous Arrival	20-May-2014	3731.26	692.00	0.7965	0.0000	0.7965	0.0000	0.0	0.0	0.0	0.0	0.0	0.0	0.0
Total															
Total										3731.26	56.6776	59.4614	6.0857		

Best objective
6.0857

MISSION SUMMARY - EEME2E31 2004 opportunity

BODY	EVENT	Date	MET	TOF	Vinfm-	Vinfm+	DeltaV	Ventry	AltFB	Altp,i	Alta,i	I,i	Altp,f	Alta,f	I,f
Earth	Departure	01-Feb-2004	0.00	0.00	0.0000	3.9017	0.0000	0.0000	0.0	0.0	0.0	0.0	0.0	0.0	0.0
Earth	- Helio centric injection	01-Feb-2004	0.00	0.00	0.0000	0.0000	3.8398	0.0000	0.0	300.0	300.0	70.1	300.0	0.0	70.1
Earth	Double hit	01-Feb-2005	365.26	365.26	3.7931	3.7963	0.0011	0.0000	1633.7	0.0	0.0	0.0	0.0	0.0	0.0
Mars	Swingby	30-Jan-2007	1094.26	729.00	8.6385	8.4384	0.1809	0.0000	1853.7	0.0	0.0	0.0	0.0	0.0	0.0
Earth	Swingby	12-Nov-2007	1380.26	286.00	8.1955	9.3396	0.9148	0.0000	12056.4	0.0	0.0	0.0	0.0	0.0	0.0
Asteroid 2	Swingby	07-Sep-2008	1680.26	300.00	8.5128	8.6784	0.2869	0.0000	0.0	0.0	0.0	0.0	0.0	0.0	0.0
Earth	Swingby	11-Nov-2009	2110.26	430.00	9.5815	9.5839	0.0017	0.0000	2696.0	0.0	0.0	0.0	0.0	0.0	0.0
Asteroid 3	Swingby	09-Jul-2010	2350.26	240.00	15.0487	15.0132	0.0615	0.0000	0.0	0.0	0.0	0.0	0.0	0.0	0.0
n/a	DSM	30-Aug-2012	3133.26	783.00	0.0000	0.0000	0.5527	0.0000	0.0	0.0	0.0	0.0	0.0	0.0	0.0
Asteroid 1	Rendezvous Arrival	27-Aug-2014	3860.26	727.00	0.6645	0.0000	0.6645	0.0000	0.0	0.0	0.0	0.0	0.0	0.0	0.0
Total															
Total										3860.26	54.5432	58.8615	6.5406		

Best objective
6.5406

MISSION SUMMARY - EEME2E31 2004 opportunity

BODY	EVENT	Date	MET	TOF	Vinfm-	Vinfm+	DeltaV	Ventry	AltFB	Altp,i	Alta,i	I,i	Altp,f	Alta,f	I,f
Earth	Departure	01-Feb-2004	0.00	0.00	0.0000	3.7931	0.0000	0.0000	0.0	0.0	0.0	0.0	0.0	0.0	0.0
Earth	- Helio centric injection	01-Feb-2004	0.00	0.00	0.0000	0.0000	3.8398	0.0000	0.0	300.0	300.0	70.1	300.0	0.0	70.1
Earth	Double hit	01-Feb-2005	365.26	365.26	3.7931	3.7963	0.0011	0.0000	1633.7	0.0	0.0	0.0	0.0	0.0	0.0
Mars	Swingby	27-Jan-2007	1090.88	725.63	8.5148	8.5650	0.0457	0.0000	2250.1	0.0	0.0	0.0	0.0	0.0	0.0
Earth	Swingby	08-Nov-2007	1376.13	285.25	8.4410	9.3988	0.7841	0.0000	14022.0	0.0	0.0	0.0	0.0	0.0	0.0
Asteroid 2	Swingby	04-Sep-2008	1676.63	300.50	8.6465	8.6455	0.0017	0.0000	0.0	0.0	0.0	0.0	0.0	0.0	0.0
Earth	Swingby	12-Nov-2009	2110.63	434.00	9.4265	9.3470	0.0564	0.0000	2810.6	0.0	0.0	0.0	0.0	0.0	0.0
Asteroid 3	Swingby	12-Jul-2010	2352.69	242.06	14.7596	14.7596	0.0000	0.0000	0.0	0.0	0.0	0.0	0.0	0.0	0.0
n/a	DSM	28-Jul-2012	3099.69	747.00	0.0000	0.0000	0.0866	0.0000	0.0	0.0	0.0	0.0	0.0	0.0	0.0
Asteroid 1	Rendezvous Arrival	15-Aug-2014	3848.19	748.50	0.7441	0.0000	0.7441	0.0000	0.0	0.0	0.0	0.0	0.0	0.0	0.0
Total															
Total										3848.19	54.3256	58.3052	5.5596		

New Horizons:

MISSION SUMMARY - EJP 2006 Opportunity

BODY	EVENT	Date	MET	TOF	Vinfm-	Vinfm+	DeltaV	Ventry	AltFB	Altp,i	Alta,i	I,i	Altp,f	Alta,f	I,f
Earth	Departure	19-Jan-2006	0.00	0.00	0.0000	12.5874	0.0000	0.0000	0.0	0.0	0.0	0.0	0.0	0.0	0.0
Earth	- Helio-centric injection	19-Jan-2006	0.00	0.00	0.0000	0.0000	8.9421	0.0000	0.0	300.0	300.0	8.9	300.0	0.0	8.9
Jupiter	Swingby	28-Feb-2007	405.00	405.00	18.5022	18.4709	0.0274	0.0000	2362696.9	0.0	0.0	0.0	0.0	0.0	0.0
Pluto	Swingby	14-Jul-2015	3463.00	3058.00	13.7888	0.0000	0.0000	0.0000	0.0	0.0	0.0	0.0	0.0	0.0	0.0

Total			3463.00	32.2910	31.0582	8.9695									

Best objective
8.9695

MISSION SUMMARY - EJP 2006 Opportunity

BODY	EVENT	Date	MET	TOF	Vinfm-	Vinfm+	DeltaV	Ventry	AltFB	Altp,i	Alta,i	I,i	Altp,f	Alta,f	I,f
Earth	Departure	19-Jan-2006	0.00	0.00	0.0000	12.7095	0.0000	0.0000	0.0	0.0	0.0	0.0	0.0	0.0	0.0
Earth	- Helio-centric injection	19-Jan-2006	0.00	0.00	0.0000	0.0000	9.0345	0.0000	0.0	300.0	300.0	9.1	300.0	0.0	9.1
Jupiter	Swingby	24-Feb-2007	401.00	401.00	18.7638	18.7638	0.0000	0.0000	2203065.8	0.0	0.0	0.0	0.0	0.0	0.0
Pluto	Swingby	26-Mar-2015	3353.71	2952.71	14.3471	0.0000	0.0000	0.0000	0.0	0.0	0.0	0.0	0.0	0.0	0.0

Total			3353.71	33.1109	31.4733	9.0345									

Best objective
9.0345

MISSION SUMMARY - EJP 2006 Opportunity

BODY	EVENT	Date	MET	TOF	Vinfm-	Vinfm+	DeltaV	Ventry	AltFB	Altp,i	Alta,i	I,i	Altp,f	Alta,f	I,f
Earth	Departure	20-Jan-2006	0.00	0.00	0.0000	12.7025	0.0000	0.0000	0.0	0.0	0.0	0.0	0.0	0.0	0.0
Earth	- Helio-centric injection	20-Jan-2006	0.00	0.00	0.0000	0.0000	9.0292	0.0000	0.0	300.0	300.0	8.9	300.0	0.0	8.9
Jupiter	Swingby	24-Feb-2007	400.08	400.08	18.7681	18.7681	0.0000	0.0000	2207920.5	0.0	0.0	0.0	0.0	0.0	0.0
Pluto	Swingby	27-Mar-2015	3352.97	2952.89	14.3459	0.0000	0.0000	0.0000	0.0	0.0	0.0	0.0	0.0	0.0	0.0

Total			3352.97	33.1140	31.4706	9.0292									

Best objective
9.0292

Voyager 2:

MISSION SUMMARY - EJSUN 1977 Opportunity

BODY	EVENT	Date	MET	TOF	Vinfm-	Vinfm+	DeltaV	Ventry	AltFB	Altp,i	Alta,i	I,i	Altp,f	Alta,f	I,f
Earth	Departure	20-Aug-1977	0.00	0.00	0.0000	10.1276	0.0000	0.0000	0.0	0.0	0.0	0.0	0.0	0.0	0.0
Earth	- Helio-centric injection	20-Aug-1977	0.00	0.00	0.0000	0.0000	7.1720	0.0000	0.0	300.0	300.0	40.9	300.0	0.0	40.9
Jupiter	Swingby	09-Jul-1979	688.00	688.00	7.8817	7.8070	0.0285	0.0000	631628.6	0.0	0.0	0.0	0.0	0.0	0.0
Saturn	Swingby	25-Aug-1981	1466.00	778.00	10.8218	10.7075	0.0506	0.0000	99201.2	0.0	0.0	0.0	0.0	0.0	0.0
Uranus	Swingby	24-Jan-1986	3079.00	1613.00	14.7495	14.7545	0.0041	0.0000	85296.5	0.0	0.0	0.0	0.0	0.0	0.0
Neptune	Swingby	25-Aug-1989	4388.00	1309.00	16.7372	0.0000	0.0000	0.0000	0.0	0.0	0.0	0.0	0.0	0.0	0.0

Total			4388.00	50.1902	43.3966	7.2552									

Best objective
7.2552

MISSION SUMMARY - EJSUN 1977 Opportunity

BODY	EVENT	Date	MET	TOF	Vinfm-	Vinfm+	DeltaV	Ventry	AltFB	Altp,i	Alta,i	I,i	Altp,f	Alta,f	I,f
Earth	Departure	02-Sep-1977	0.00	0.00	0.0000	9.4063	0.0000	0.0000	0.0	0.0	0.0	0.0	0.0	0.0	0.0
Earth	- Helio-centric injection	02-Sep-1977	0.00	0.00	0.0000	0.0000	6.6913	0.0000	0.0	300.0	300.0	31.2	300.0	0.0	31.2
Jupiter	Swingby	02-Aug-1979	699.48	699.48	7.4977	7.4977	0.0000	0.0000	739024.4	0.0	0.0	0.0	0.0	0.0	0.0
Saturn	Swingby	14-Oct-1981	1503.71	804.23	10.2361	10.2361	0.0000	0.0000	115495.3	0.0	0.0	0.0	0.0	0.0	0.0
Uranus	Swingby	21-Apr-1986	3153.71	1650.00	14.2168	14.2168	0.0000	0.0000	102316.1	0.0	0.0	0.0	0.0	0.0	0.0
Neptune	Swingby	26-Dec-1989	4498.73	1345.02	16.1304	0.0000	0.0000	0.0000	0.0	0.0	0.0	0.0	0.0	0.0	0.0

Total			4498.73	48.0809	41.3568	6.6913									

Best objective
6.6913

MISSION SUMMARY - EJSUN 1977 opportunity

BODY	EVENT	Date	MET	TOF	Vinfm-	Vinfm+	DeltaV	Ventry	AltFB	Altp,i	Alta,i	I,i	Altp,f	Alta,f	I,f
Earth	Departure	01-Sep-1977	0.00	0.00	0.0000	9.4062	0.0000	0.0000	0.0	0.0	0.0	0.0	0.0	0.0	0.0
Earth	- Helio-centric injection	01-Sep-1977	0.00	0.00	0.0000	0.0000	6.6913	0.0000	0.0	300.0	300.0	31.3	300.0	0.0	31.3
Jupiter	Swingby	02-Aug-1979	699.53	699.53	7.4977	7.4977	0.0000	0.0000	738931.5	0.0	0.0	0.0	0.0	0.0	0.0
Saturn	Swingby	14-Oct-1981	1503.75	804.22	10.2364	10.2364	0.0000	0.0000	115484.5	0.0	0.0	0.0	0.0	0.0	0.0
Uranus	Swingby	21-Apr-1986	3153.73	1649.98	14.2170	14.2170	0.0000	0.0000	102307.9	0.0	0.0	0.0	0.0	0.0	0.0
Neptune	Swingby	26-Dec-1989	4498.74	1345.00	16.1307	0.0000	0.0000	0.0000	0.0	0.0	0.0	0.0	0.0	0.0	0.0

Total			4498.74	48.0818	41.3573	6.6913									

Best objective
6.6913

Galileo:

MISSION SUMMARY - EVE1E2J 1989 Opportunity

BODY	EVENT	Date	MET	TOF	vinfm-	vinfm+	DeltaV	Ventry	AltFB	Altp,i	Alta,i	I,i	Altp,f	Alta,f	I,f
Earth	Departure	18-Oct-1989	0.00	0.00	0.0000	3.9326	0.0000	0.0000	0.0	0.0	0.0	0.0	0.0	0.0	0.0
Earth	- Helio-centric injection	18-Oct-1989	0.00	0.00	0.0000	0.0000	3.8863	0.0000	0.0	300.0	300.0	12.7	300.0	0.0	12.7
Venus	Swingby	10-Feb-1990	115.00	115.00	6.1994	5.9786	0.1649	0.0000	16049.0	0.0	0.0	0.0	0.0	0.0	0.0
Earth	Swingby	08-Dec-1990	416.00	301.00	8.7923	8.9879	0.1291	0.0000	1396.9	0.0	0.0	0.0	0.0	0.0	0.0
Asteroid 1	Swingby	29-Oct-1991	0.00	325.00	6.1994	6.0094	0.1242	0.0000	0.0	0.0	0.0	0.0	0.0	0.0	0.0
Earth	Swingby	08-Dec-1992	1147.00	406.00	8.8232	8.8227	0.0003	0.0000	668.4	0.0	0.0	0.0	0.0	0.0	0.0
Asteroid 2	Swingby	28-Aug-1993	1410.00	263.00	12.4480	12.5795	0.2277	0.0000	0.0	0.0	0.0	0.0	0.0	0.0	0.0
Jupiter	- Target orbit insertion	07-Dec-1995	2241.00	831.00	0.0000	0.0000	0.7417	0.0000	0.0	214500.0	0.0	5.3	214500.0	21000000.0	5.3
Jupiter	Arrival	07-Dec-1995	2241.00	0.00	5.7049	0.0000	0.0000	0.0000	0.0	0.0	0.0	0.0	0.0	0.0	0.0
Total				2241.00	49.9939	48.2526	5.2794								

Best objective
5.2794

MISSION SUMMARY - EVE1E2J 1989 opportunity

BODY	EVENT	Date	MET	TOF	vinfm-	vinfm+	DeltaV	Ventry	AltFB	Altp,i	Alta,i	I,i	Altp,f	Alta,f	I,f
Earth	Departure	18-Oct-1989	0.00	0.00	0.0000	3.9326	0.0000	0.0000	0.0	0.0	0.0	0.0	0.0	0.0	0.0
Earth	- Helio-centric injection	18-Oct-1989	0.00	0.00	0.0000	0.0000	3.8863	0.0000	0.0	300.0	300.0	12.7	300.0	0.0	12.7
Venus	Swingby	10-Feb-1990	115.00	115.00	6.1994	6.0094	0.1242	0.0000	16083.1	0.0	0.0	0.0	0.0	0.0	0.0
Earth	Swingby	08-Dec-1990	416.27	301.27	8.8105	8.8363	0.0170	0.0000	1378.0	0.0	0.0	0.0	0.0	0.0	0.0
Asteroid 1	Swingby	03-Nov-1991	746.23	329.95	7.7437	7.9994	0.4428	0.0000	0.0	0.0	0.0	0.0	0.0	0.0	0.0
Earth	Swingby	07-Dec-1992	1146.32	400.10	9.0362	8.7948	0.1526	0.0000	300.1	0.0	0.0	0.0	0.0	0.0	0.0
Asteroid 2	Swingby	29-Aug-1993	1411.32	265.00	12.3260	12.3260	0.0001	0.0000	0.0	0.0	0.0	5.3	0.0	0.0	0.0
Jupiter	- Target orbit insertion	16-Jan-1996	2281.04	869.77	0.0000	0.0000	0.7240	0.0000	0.0	214500.0	0.0	5.3	214500.0	21000000.0	5.3
Jupiter	Arrival	16-Jan-1996	2281.04	0.00	5.6101	0.0000	0.0000	0.0000	0.0	0.0	0.0	0.0	0.0	0.0	0.0
Total				2281.04	49.7259	47.8986	5.3649								

Best objective
5.3649

MISSION SUMMARY - EVE1E2J 1989 Opportunity

BODY	EVENT	Date	MET	TOF	vinfm-	vinfm+	DeltaV	Ventry	AltFB	Altp,i	Alta,i	I,i	Altp,f	Alta,f	I,f
Earth	Departure	20-Oct-1989	0.00	0.00	0.0000	3.8659	0.0000	0.0000	0.0	0.0	0.0	0.0	0.0	0.0	0.0
Earth	- Helio-centric injection	20-Oct-1989	0.00	0.00	0.0000	0.0000	3.8639	0.0000	0.0	300.0	300.0	14.8	300.0	0.0	14.8
Venus	Swingby	12-Feb-1990	115.75	115.75	5.8309	5.8159	0.0111	0.0000	16566.8	0.0	0.0	0.0	0.0	0.0	0.0
Earth	Swingby	11-Dec-1990	417.00	301.25	8.7829	8.7522	0.0197	0.0000	897.3	0.0	0.0	0.0	0.0	0.0	0.0
Asteroid 1	Swingby	01-Nov-1991	742.00	325.00	7.9466	7.9454	0.0021	0.0000	0.0	0.0	0.0	0.0	0.0	0.0	0.0
Earth	Swingby	08-Dec-1992	1145.75	403.75	8.8216	8.7194	0.0641	0.0000	348.3	0.0	0.0	0.0	0.0	0.0	0.0
Asteroid 2	Swingby	30-Aug-1993	1410.50	264.75	12.2677	12.2677	0.0000	0.0000	0.0	0.0	0.0	0.0	0.0	0.0	0.0
Jupiter	- Target orbit insertion	29-Jan-1996	2292.00	881.50	0.0000	0.0000	0.7213	0.0000	0.0	214500.0	0.0	5.3	214500.0	21000000.0	5.3
Jupiter	Arrival	29-Jan-1996	2292.00	0.00	5.5955	0.0000	0.0000	0.0000	0.0	0.0	0.0	0.0	0.0	0.0	0.0
Total				2292.00	49.2453	47.3665	4.6822								

Best objective
4.6822

Cassini:

MISSION SUMMARY - EVEJ5 1997 Opportunity

BODY	EVENT	Date	MET	TOF	vinfm-	vinfm+	DeltaV	Ventry	AltFB	Altp,i	Alta,i	I,i	Altp,f	Alta,f	I,f
Earth	Departure	07-Oct-1997	0.00	0.00	0.0000	4.0427	0.0000	0.0000	0.0	0.0	0.0	0.0	0.0	0.0	0.0
Earth	- Helio-centric injection	07-Oct-1997	0.00	0.00	0.0000	0.0000	3.9241	0.0000	0.0	300.0	300.0	5.7	300.0	0.0	5.7
Venus	Swingby	22-Apr-1998	197.00	197.00	6.1376	6.1380	0.0002	0.0000	300.0	0.0	0.0	0.0	0.0	0.0	0.0
n/a	DSM	27-Oct-1998	384.50	187.50	0.0000	0.0000	0.4509	0.0000	0.0	0.0	0.0	0.0	0.0	0.0	0.0
Venus	Swingby	21-Jun-1999	622.00	237.50	9.2018	9.2019	0.0001	0.0000	2299.3	0.0	0.0	0.0	0.0	0.0	0.0
Earth	Swingby	17-Aug-1999	679.00	57.00	15.7395	15.8446	0.0870	0.0000	614.3	0.0	0.0	0.0	0.0	0.0	0.0
Jupiter	Swingby	31-Dec-2000	1181.00	502.00	10.5578	10.4756	0.0750	0.0000	11227388.4	0.0	0.0	0.0	0.0	0.0	0.0
Saturn	- Target orbit insertion	02-Jul-2004	2460.00	1279.00	0.0000	0.0000	0.5872	0.0000	0.0	20000.0	0.0	16.0	20000.0	10000000.0	16.0
Saturn	Arrival	02-Jul-2004	2460.00	0.00	5.3690	0.0000	0.0000	0.0000	0.0	0.0	0.0	0.0	0.0	0.0	0.0
Total				2460.00	47.0058	45.7029	5.1244								

Best objective
5.1244

MISSION SUMMARY - EVEJ5 1997 Opportunity

BODY	EVENT	Date	MET	TOF	vinfm-	vinfm+	DeltaV	Ventry	AltFB	Altp,i	Alta,i	I,i	Altp,f	Alta,f	I,f
Earth	Departure	04-Nov-1997	0.00	0.00	0.0000	2.9474	0.0000	0.0000	0.0	0.0	0.0	0.0	0.0	0.0	0.0
Earth	- Helio-centric injection	04-Nov-1997	0.00	0.00	0.0000	0.0000	3.5907	0.0000	0.0	300.0	300.0	3.7	300.0	0.0	3.7
Venus	Swingby	23-Apr-1998	170.00	170.00	5.1572	6.1713	0.5999	0.0000	4879.7	0.0	0.0	0.0	0.0	0.0	0.0
n/a	DSM	19-Jun-1999	624.96	205.87	8.8292	9.2734	0.3245	0.0000	0.0	0.0	0.0	0.0	0.0	0.0	0.0
Venus	Swingby	18-Jun-1999	591.75	207.25	9.2768	9.2706	0.0047	0.0000	3525.9	0.0	0.0	0.0	0.0	0.0	0.0
Earth	Swingby	16-Aug-1999	650.75	59.00	15.5925	15.6100	0.0143	0.0000	302.7	0.0	0.0	0.0	0.0	0.0	0.0
Jupiter	Swingby	09-Jan-2001	1162.75	512.00	10.2734	10.2726	0.0007	0.0000	10443678.3	0.0	0.0	0.0	0.0	0.0	0.0
Saturn	- Target orbit insertion	21-Sep-2004	2513.75	1351.00	0.0000	0.0000	0.5530	0.0000	0.0	20000.0	0.0	15.6	20000.0	10000000.0	15.6
Saturn	Arrival	21-Sep-2004	2513.75	0.00	5.1668	0.0000	0.0000	0.0000	0.0	0.0	0.0	0.0	0.0	0.0	0.0
Total				2513.75	45.4668	44.2720	5.1838								

Best objective
5.1838

MISSION SUMMARY - EVEJ5 1997 Opportunity

BODY	EVENT	Date	MET	TOF	vinfm-	vinfm+	DeltaV	Ventry	AltFB	Altp,i	Alta,i	I,i	Altp,f	Alta,f	I,f
Earth	Departure	02-Oct-1997	0.00	0.00	0.0000	3.8895	0.0000	0.0000	0.0	0.0	0.0	0.0	0.0	0.0	0.0
Earth	- Helio-centric injection	02-Oct-1997	0.00	0.00	0.0000	0.0000	3.8718	0.0000	0.0	300.0	300.0	10.3	300.0	0.0	10.3
Venus	Swingby	16-Apr-1998	196.00	196.00	5.7875	6.1055	0.1612	0.0000	301.0	0.0	0.0	0.0	0.0	0.0	0.0
n/a	DSM	26-Nov-1998	419.09	223.09	0.0000	0.0000	0.3869	0.0000	0.0	0.0	0.0	0.0	0.0	0.0	0.0
Venus	Swingby	19-Jun-1999	624.96	205.87	8.8292	9.2734	0.3245	0.0000	4347.2	0.0	0.0	0.0	0.0	0.0	0.0
Earth	Swingby	16-Aug-1999	682.98	58.02	15.7061	15.7063	0.0002	0.0000	350.5	0.0	0.0	0.0	0.0	0.0	0.0
Jupiter	Swingby	01-Jan-2001	1186.98	504.00	10.5081	10.5080	0.0001	0.0000	11239611.2	0.0	0.0	0.0	0.0	0.0	0.0
Saturn	- Target orbit insertion	29-Jun-2004	2461.18	1274.20	0.0000	0.0000	0.5913	0.0000	0.0	20000.0	0.0	16.0	20000.0	10000000.0	16.0
Saturn	Arrival	29-Jun-2004	2461.18	0.00	5.3929	0.0000	0.0000	0.0000	0.0	0.0	0.0	0.0	0.0	0.0	0.0
Total				2461.18	46.2239	45.4827	5.3459								

Best objective
5.3459

REPORT DOCUMENTATION PAGE

*Form Approved
OMB No. 0704-0188*

The public reporting burden for this collection of information is estimated to average 1 hour per response, including the time for reviewing instructions, searching existing data sources, gathering and maintaining the data needed, and completing and reviewing the collection of information. Send comments regarding this burden estimate or any other aspect of this collection of information, including suggestions for reducing this burden, to Department of Defense, Washington Headquarters Services, Directorate for Information Operations and Reports (0704-0188), 1215 Jefferson Davis Highway, Suite 1204, Arlington, VA 22202-4302. Respondents should be aware that notwithstanding any other provision of law, no person shall be subject to any penalty for failing to comply with a collection of information if it does not display a currently valid OMB control number.
PLEASE DO NOT RETURN YOUR FORM TO THE ABOVE ADDRESS.

1. REPORT DATE (DD-MM-YYYY) 01-07-2014		2. REPORT TYPE Technical Memorandum		3. DATES COVERED (From - To)	
4. TITLE AND SUBTITLE Design of the VISITOR Tool: A Versatile ImpulSive Interplanetary Trajectory OptimizeR				5a. CONTRACT NUMBER	
				5b. GRANT NUMBER	
				5c. PROGRAM ELEMENT NUMBER	
6. AUTHOR(S) Corpaccioli, Luca; Linskens, Harry; Komar, David R.				5d. PROJECT NUMBER	
				5e. TASK NUMBER	
				5f. WORK UNIT NUMBER 662122.04.07.16	
7. PERFORMING ORGANIZATION NAME(S) AND ADDRESS(ES) NASA Langley Research Center Hampton, VA 23681-2199				8. PERFORMING ORGANIZATION REPORT NUMBER L-20442	
9. SPONSORING/MONITORING AGENCY NAME(S) AND ADDRESS(ES) National Aeronautics and Space Administration Washington, DC 20546-0001				10. SPONSOR/MONITOR'S ACRONYM(S) NASA	
				11. SPONSOR/MONITOR'S REPORT NUMBER(S) NASA/TM-2014-218509	
12. DISTRIBUTION/AVAILABILITY STATEMENT Unclassified - Unlimited Subject Category 13 Availability: NASA CASI (443) 757-5802					
13. SUPPLEMENTARY NOTES					
14. ABSTRACT The design of trajectories for interplanetary missions represents one of the most complex and important problems to solve during conceptual space mission design. To facilitate conceptual mission sizing activities, it is essential to obtain sufficiently accurate trajectories in a fast and repeatable manner. To this end, the VISITOR tool was developed. This tool modularly augments a patched conic MGA-1DSM model with a mass model, launch window analysis, and the ability to simulate more realistic arrival and departure operations. This was implemented in MATLAB, exploiting the built-in optimization tools and vector analysis routines. The chosen optimization strategy uses a grid search and pattern search, an iterative variable grid method. A genetic algorithm can be selectively used to improve search space pruning, at the cost of losing the repeatability of the results and increased computation time. The tool was validated against seven flown missions: the average total mission ζV offset from the nominal trajectory was 9.1%, which was reduced to 7.3% when using the genetic algorithm at the cost of an increase in computation time by a factor 5.7.					
15. SUBJECT TERMS Astrodynamics; Deep space maneuver; Gravity assist; Interplanetary; Lambert; Mission design; Optimization					
16. SECURITY CLASSIFICATION OF:			17. LIMITATION OF ABSTRACT	18. NUMBER OF PAGES	19a. NAME OF RESPONSIBLE PERSON
a. REPORT	b. ABSTRACT	c. THIS PAGE			STI Help Desk (email: help@sti.nasa.gov)
U	U	U	UU	40	19b. TELEPHONE NUMBER (Include area code) (443) 757-5802